Marielies Reiter, BSc

Effects of HDL3 and Apolipoprotein A-I on Amyloid-beta Production and its Transport at the Blood-Brain Barrier

MASTER'S THESIS

to achieve the university degree of

Master of Science

Master's degree programme: Molecular Microbiology

submitted to

Graz University of Technology

Supervisor

Assoc.Prof. PD Mag. Dr.rer.nat. Ute Panzenböck

Institute of Pathophysiology and Immunology
Medical University Graz
Optional field (second supervisor/name of the faculty, etc.)
max 2 lines

Graz, April 2016

AFFIDAVIT

I declare that I have authored this thesis independently, that I have not used other than the declared sources/resources, and that I have explicitly indicated all material which has been quoted either literally or by content from the sources used. The text document uploaded to TUGRAZonline is identical to the present master‘s thesis dissertation.

28.04.2016

Date

Signature

Acknowledgement

I would first like to thank my supervisor Assoc. Prof. PD Mag. Dr.rer.nat Ute Panzenböck for supporting and helping me during my research and granting me the opportunity of writing my thesis over such an interesting topic.

Special thanks to Chaitanya Chakravarthi Gali, Nicole Maria Albrecher and my entire working group for not only offering their help and support, but also for becoming sincere friends who cheered me up during hard times and made me laugh whenever they could. It was an honor being a part of your team.

Last but not least, I would like to thank my family and friends who have supported me any and every way they could, not only during my master's thesis but throughout my entire life. Without you, I would never have become the person I am today and I call myself lucky and proud to have every single one of you in my life.

Abstract

Alzheimer's disease (AD) is the most prevalent form of dementia worldwide, with an estimated 135,5 million people becoming affected by the year 2050. Although the discovery of the disease was more than a century ago, there is still no promising treatment available. The difficulty in developing such treatments is attributed to the fact that AD is still not sufficiently understood. Researchers have developed various hypotheses, but the topic remains controversial. It is generally accepted that the amyloid-beta peptide (Aβ) plays an important role in the progression of the disease. An accumulation of this peptide leads to extracellular plaque formation, first discovered by Alzheimer in 1906. In addition, the outcome of several previous studies established an association between Aβ and lipid / lipoprotein metabolism. In this thesis, the effect of the lipoprotein HDL_3 and its main apolipoprotein A-I (apoA-I) on the Aβ precursor protein (APP) expression and processing as well as Aβ transport at the blood-brain barrier (BBB) is investigated using a well established *in vitro* model consisting of primary porcine brain capillary endothelial cells (pBCEC). Furthermore, the impact of Aβ on apoA-I and HDL function is examined. Since both, HDL_3 and apoA-I were already shown to prevent formation of reactive oxygen species (ROS) in other tissues and, thus, preventing oxidative stress and associated cell damage, it was not surprising that we could prove this to apply also in pBCEC. Interestingly, both, HDL_3 and Aβ promote expression of APP, although it is presently unclear how APP is further processed. While in pBCEC mainly HDL_3 promotes cholesterol efflux, the presence of $Aβ_{1-40}$ had no impact on efflux, however, when combined with HDL_3 $Aβ_{1-40}$ showed increased levels of the two transporters low density lipoprotein receptor related protein 1 (LRP1) and ATP binding cassette transporter (ABC) G1, the former known to promote Aβ clearance from the brain. Additionally, HDL_3 led to higher extracellular Aβ oligomer levels, identified as pre-fibrils, 2.4-fold, in combination with $Aβ_{1-40}$ peptides even 3.6-fold, letting us infer that HDL_3 may act as a chaperone and contribute to Aβ clearance from the brain. Whether this effect occurs by directly binding Aβ peptides or by stimulating other pathways has yet not been understood. Transport studies to confirm this clearance hypothesis revealed not convincing. However, we were able to demonstrate that apoA-I is capable of counteracting Aβ uptake.

The results obtained provide a good basis for further studies, which are urgently needed to gain deeper insights into the connection between APP, Aβ and HDL_3 / apoA-I at the interface between the central nervous system (CNS) and the circulation.

Zusammenfassung

Die Alzheimer Krankheit ist die wohl weitverbreitetste Demenzerkrankung weltweit, mit etwa 135,5 Millionen Betroffenen im Jahre 2050. Obwohl die Krankheit bereits vor über hundert Jahren entdeckt wurde, gibt es noch keine vielversprechenden Behandlungsmethoden. Die Schwierigkeit hierbei liegt vermutlich daran, dass die Pathogenese der Alzheimer Erkrankung bis heute nicht ausreichend verstanden wird. Über die Jahre haben Forscher verschiedenste Hypothesen aufgestellt und die Literatur dazu ist häufig kontrovers. Weitgehend anerkannt wird jedoch, dass das toxische Amyloid-beta Peptid (Aβ) eine wichtige Rolle im Verlauf der Krankheit spielt. Bei einer Anhäufung dieses Peptids im extrazellulären Bereich des Gehirns kann es sogenannte Plaques bilden, welche bereits 1906 von Alzheimer bei der Entdeckung der Krankheit nachgewiesen wurden. Darüberhinaus konnten schon vorhergehende Studien einen Zusammenhang zwischen Aβ und dem Lipid- und Lipoproteinstoffwechsel herstellen. In dieser Arbeit wird die Auswirkung des Lipoproteins HDL_3 und seinem Haupt-Apolipoprotein A-I (apoA-I) auf die Expression von Amyloid Precursor Protein (APP) und dessen „Processing“ sowie der Transport von Aβ an der Blut-Hirn Schranke anhand eines gut etablierten *in vitro* Modells aus primären Schweinehirn-Kapillarendothelzellen (pBCEC) untersucht. Zudem soll der Einfluss von Aβ auf die Funktionen von apoA-I und HDL anhand dieser Zellen erforscht werden. Dass sowohl HDL_3 als auch apoA-I die Bildung der „Reaktiven Sauerstoff-Spezies“ (ROS) verhindern und so oxidativem Stress und den damit verbundenen Zellschäden vorbeugen, konnte bereits in anderem Gewebe nachgewiesen werden, weshalb es nicht überraschend war, dass dies auch für unsere pBCEC zutraf. Interessanterweise steigert die Behandlung der Zellen mit sowohl HDL_3 als auch Aβ die Expression des Aβ-Vorläuferproteins APP, jedoch ist bisher unklar, wie APP schließlich weiter gespalten wird. In pBCEC ist HDL_3 Hauptverursacher des Cholesterin Efflux. Unsere Untersuchungen ergaben, dass Aβ hierbei keinen Einfluss hatte, jedoch in Kombination mit HDL_3 zu erhöhten mRNA Levels der beiden Transporter „low density lipoprotein receptor related protein 1“ (LRP1) und „ATP binding cassette transporter“ (ABC) G1 führte, wobei LRP1 nachweislich zur Beseitigung von Aβ aus dem Hirn beiträgt. Zusätzlich steigerte HDL_3 extrazelluläre Aβ Oligomer Levels um ein 2,4-faches, in Kombination mit $Aβ_{1-40}$ Peptiden sogar um ein 3,6-faches. Diese Beobachtungen lassen uns vermuten, dass HDL_3 als Chaperon wirken und an der Beseitigung von Aβ aus dem Hirn beteiligt sein könnte. Ob dies

über direktes Binden der Aβ-Peptide oder durch Aktivierung weiterer Signalwege geschieht, ist unklar. Auch Transport-Studien, die diese Hypothese bestätigten könnten, waren wenig aufschlussreich. Jedoch konnten wir zeigen, dass apoA-I in der Lage ist, der Aβ-Aufnahme von pBCEC entgegenzuwirken.

Die Ergebnisse dieser Arbeit liefern eine gute Basis für weitere Experimente, die dringend benötigt werden, um den Zusammenhang zwischen APP, Aβ und HLD_3 / apoA-I an der Schnittstelle zwischen Zentralnervensystem und dem Blutkreislauf besser zu verstehen.

Table of contents

List of Abbreviations

Aβ	amyloid-beta peptide
ABC	ATP binding cassette transporter
ACAT	acetyl-coenzymeA:cholesterol acyltransferase
AD	Alzheimer's disease
ADAM	a disintegrin and metalloproteinase
apo	apolipoprotein
APP	amyloid-beta precursor protein
BACE	β-site of APP cleaving enzyme
BBB	blood-brain barrier
CNS	central nervous system
(p)BCEC	(porcine) brain capillary endothelial cells
HDL	high density lipoproteins
HDL-C	HDL-cholesterol
LRP	low density lipoprotein receptor related protein
LCAT	lecithin–cholesterol acyltransferase
LXR	liver-X receptor
NFT	neurofibrillary tangles
RAGE	receptor for advanced glycation endproducts
ROS	reactive oxygen species
TEER	transendothelial electrical resistance
qRT-PCR	quantitative real time polymerase chain reaction

1. Introduction

Over 47.5 million people suffer from dementia worldwide, with around 7.7 million new cases being reported each year. The numbers are rapidly increasing and by the year 2050 even 135.5 million people are expected to have this syndrome. Alzheimer's disease (AD) is the most common form, with an estimated number of 60-70% of all dementia related cases resulting in this specific disease.[1]

AD was named after the German neuropathologist Alois Alzheimer, who in 1906, was the first to discover and describe two neuropathological abnormalities, later identified as senile plaques and neurofibrillary tangles (NFT), in a 51 year old patient showing signs of cognitive impairment.[2,3] Although this discovery occurred more than a century ago, no effective treatments to prevent, halt, or reverse this neurodegenerative disorder have been established so far.[4]

AD can be classified into early-onset AD, manifesting in individuals between 30 and 60 years (~1-6%), and late-onset AD, diagnosed in patients at the age of 60 and older (~90%). Thus, the greatest risk factor for developing AD is advancing age,[5,6] but the etiology of the disease is multifactorial and complex.[7,8] Diabetes mellitus, female gender, head trauma, hyperlipidemia, positive family history, previous depression and vascular factors also increase the chances of contracting AD.[6] The consequences are loss of synapses and neurons, as well as formation of extracellular senile plaques and intracellular neurofibrillary tangles.[9] Affected people suffer symptoms such as progressive decline in cognitive function, which are often accompanied with behavioral disturbances.[10]

Although it is now widely accepted that amyloid-beta peptides (Aβ) play a key role in the pathogenesis of the disorder,[11] the exact mechanisms are still poorly understood and additional research is required.[12]

1.1. Amyloid-beta peptide

According to various prior studies, Aβ plays a crucial role in the progression of AD. The amyloid-beta precursor protein (APP) can be processed in two different signaling pathways by distinctive, proteolytic cleavage of secretases. While for the non-amyloidogenic pathway APP cleavage by α-secretases, members of the ADAM

family, leads to release of soluble APPα (sAPPα) having neuroprotective properties, sequential cleavage by β-secretase (BACE1) and γ-secretase complex leads towards the amyloidogenic pathway releasing sAPPβ and Aβ,[13–15] (shown in Figure 1).[15] The amyloid cascade hypothesis suggests that predominant cleavage by β-secretase is causing an imbalance of Aβ peptide production and clearance, which further leads to spontaneous aggregation of the peptide into soluble oligomers. Those then are capable to form fibrils and might even deposit in diffuse senile plaques.[12,16,17] Whether the formation of senile plaques is one of the reasons causing AD or just a by-product of the disease is not completely understood.[18] Also, the relationship between senile plaques and NFT is still unclear, although previous studies suggest that Aβ fibrils induce tau phosphorylation.[19,20]

It is generally accepted that the two major isoforms of Aβ, $Aβ_{1-40}$ and $Aβ_{1-42}$ containing 40 and 42 amino acids, respectively, are toxic and contribute to synaptic and mitochondrial damage as well as increased release of ROS.[21,22] The most abundant isoform in the brain is $Aβ_{1-40,}$[23] but $Aβ_{1-42}$ has two additional amino acids, making it more hydrophobic and, thus, it is more likely for $Aβ_{1-42}$ to aggregate.[24]

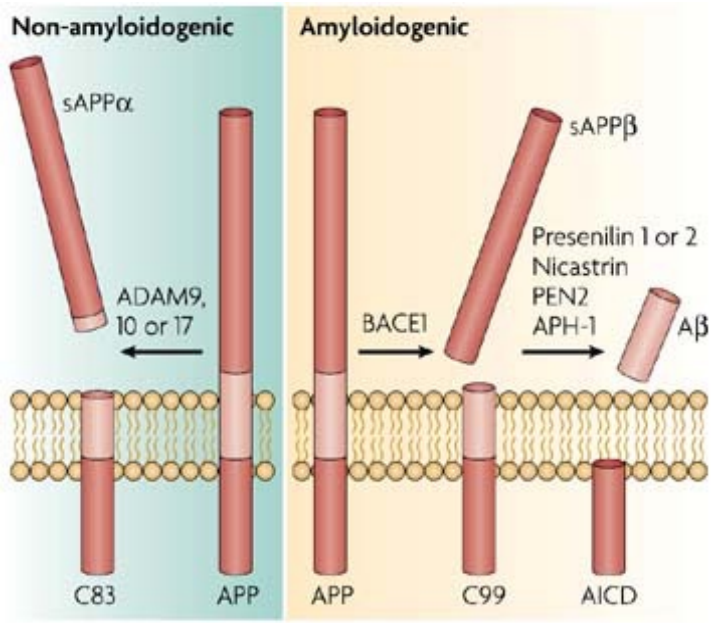

Figure 1: APP processing into two different signaling pathways. Cleavage of APP by α-secretases, ADAM9, 10 or 17, leads towards the non-amyloidogenic pathway and formation and release of sAPPα. Proteolytic processing through the amyloidogenic pathway occurs when APP is cleaved by the β-secretase (BACE1) and γ-secretase complex into sAPPβ, Aβ and the amyloid precursor protein intracellular domain (AICD). Aβ and sAPPβ are released. (Figure adapted from LaFerla *et al.*[15])

1.1.1. Aβ and reactive oxygen species

The term reactive oxygen species (ROS) summarizes oxygen molecules with an unpaired electron rendering them extremely reactive, such as superoxide, hydrogen peroxide, singlet oxygen, ozone, hypohalous acids, and organic peroxides.[25] ROS production occurs during normal cell metabolism in multiple cell compartments and is very complex. An overproduction results in "oxidative stress",[26] further causing damage to biomolecules, such as lipids, proteins, and DNA, and might even lead to chronic diseases.[27] In the past, ROS have been noticed to be an important factor in the pathogenesis of AD. Consistently, increased ROS levels were associated with accumulation of Aβ peptides and Aβ was proven to promote formation of hydrogen peroxides and lipid peroxides.[28–33] On the other hand, Behl *et al.* suggested that the toxicity of Aβ results from the free radical damage of hydrogen peroxides.[34] It is hypothesized that there is a connection between Aβ, ROS, and the nuclear factor NF-κB, known to be a regulator of ROS,[35] but to fully understand this pathway, further research is required.

1.1.2. Aβ transport and clearance

Besides NFT, Aβ plaques are one of the two main hallmarks of AD and several prior studies have shown that increased failure of Aβ clearance is recognized in the pathogenesis of the disease.[24] Soluble, extracellular Aβ in the brain is removed mainly across the BBB.[24,36] The apical side facing the blood circulation and the basolateral side facing the brain parenchyma are functionally distinct.[37] Transport across the BBB is generally restricted to molecular weight, diameter and solubility of proteins.[38] Although Aβ peptides are generally small enough to cross the BBB, tight junctions between the cells prevent them from passing the BBB, so they therefore require special transporters.[24] In contrast, a disrupted BBB allows circulating Aβ to pass the barrier.[39] Recent *in vitro* and *in vivo* studies identified the low density lipoprotein receptor related protein-1 (LRP1) to promote clearance of Aβ across the BBB and, hence, prevent the accumulation, aggregation, and deposition of Aβ peptides.[40,41] While the ATP-binding cassette transporter (ABC) B1 directly exports Aβ into the circulation, ABCA1, earlier shown by our group to be preferentially located at the basolateral side of the BBB,[42] indirectly promotes Aβ clearance.[43] The exact mechanism however is yet not understood, but Tokuda *et al.* suggest that by regulating cholesterol efflux, also lipid levels of apoE are controlled. Higher lipidated

apoE then can bind Aβ more efficiently, thus, modulating the capacity of Aβ to aggregate.[44]

On the other hand, receptor for advanced glycation endproducts (RAGE) can transport Aβ from the circulation into the brain, although this event is mostly inhibited by soluble transporters, such as soluble form of RAGE, soluble form of LRP, anti-Aβ IgG and serum amyloid P component, which bind 70-90% of plasma Aβ.[24]

1.2. The Role of Cholesterol and (Apo)Lipoproteins in AD

In 1911, Alzheimer discovered uncommon lipid changes in the brain of an AD patient.[45] Only decades later researchers established a link between lipid metabolism and AD, when apolipoprotein E (apoE) type 4 allele was identified as a strong risk factor for late-onset AD.[9,46,47] Whether apoE4 contributes to loss of neuroprotective function or gain of toxic function is discussed very controversially in the literature.[48,49]

By now, researchers have revealed that cholesterol metabolism is associated with AD. Cholesterol is a multifaceted molecule. It acts as a cofactor for signaling molecules, as a precursor for steroid hormones, VitD, and bile acids, and, not least, is an essential component of cellular membranes determining their fluidity and biophysical properties by lowering permeability and increasing compacity.[50,51] The most cholesterol-rich organ of the human is the brain with about 25% of the total amount in the human body.[52] There, the lipid is mainly synthesized *de novo* by astrocytes, oligodentrocytes, and neurons. Degenerating neurons and synapses increase the release of cholesterol in AD.[53] To maintain cholesterol levels sensed through the membrane-bound sterol regulatory element-binding protein (SREBP),[54] cholesterol is catabolized to 24*S*-hydroxycholesterol (24*S*-OHC) via cholesterol 24-hydroxylase, CYP46A1,[55] and then transported across the BBB into the circulation where it is transferred and finally eliminated in the liver.[56] Else, 24*S*-OHC can also act as a ligand of liver-X receptors (LXR) α and β, which have the ability to regulate gene expression of various proteins involved in cholesterol metabolism.[57] Results from our group have shown that in pBCEC, LXR activate cholesterol efflux via ABCA1 and apoA-I.[58] ABCA1 promotes cholesterol efflux towards apoA-I, leading to HDL generation, and ABCG1 towards HDL,[59,60] as illustrated in Figure 2.[61] Cholesterol transport from the peripheral circulation into the brain is usually

prevented by an intact BBB.[53] While cholesterol in the brain is mainly unesterified, the enzyme acetyl-coenzymeA:cholesterol acyltransferase (ACAT) can convert the unesterified membrane cholesterol into cytoplasmic cholesteryl-ester droplets for storage and, hence, regulates intracellular cholesterol homeostasis.[9,62,63] Interestingly, numerous studies reported that inhibition of ACAT results in decrease of Aβ production and increase of Aβ clearance.[63–67] The influence of cholesterol on Aβ production might further be attributed to the fact that cholesterol affects the membrane properties. Higher cholesterol content in lipid rafts allows clustering of the membrane-associated β- and γ-secretases with their substrates, thus, promoting the pathogenic cleavage of APP into Aβ.[9]

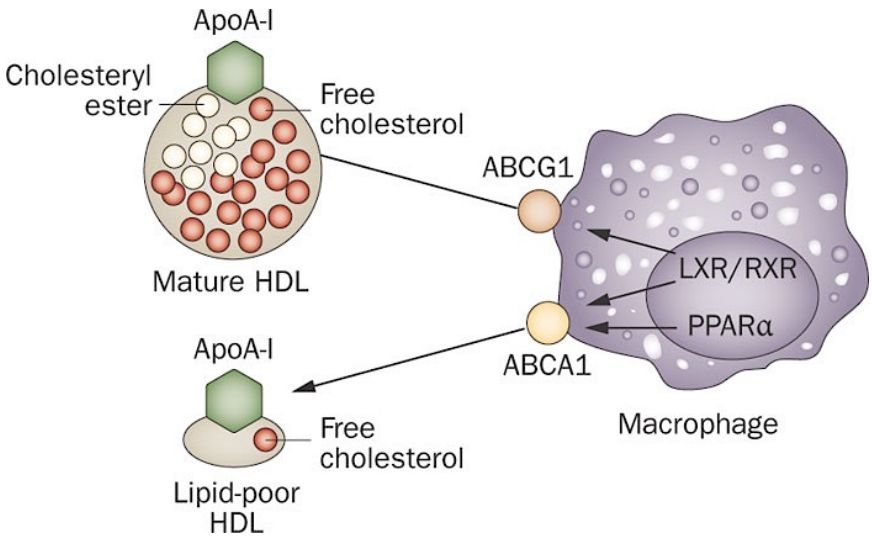

Figure 2: Free cholesterol transport. ABCA1 promotes the transport of free cholesterol towards lipid-poor apoA-I, ABCG1 towards mature HDL, here shown on a macrophage model. (Figure adapted from Duffy and Rader. [61])

1.2.1. High-density lipoproteins

High-density lipoproteins (HDL) are plurimolecluar particles predominantly consisting of polar lipids solubilized by apolipoproteins. In addition HDL carry many different proteins. The main protein components of HDL include apolipoproteins and enzymes, recognized as key components, but also proteins of acute-phase response, complement regulation, proteinase inhibition, immune response and hemostasis. HDL molecules are highly heterogeneous in their structural, chemical and biological properties and exist in multiple isoforms. There are two main subclasses: a less dense HDL_2 and a protein-richer HDL_3 with higher density.[68] These two subclasses can be separated by ultracentrifugation, as described in "3.2. Isolation". ApoA-I is believed to be present in almost all HDL particles and accounts for approximately 70% of total HDL protein. Further HDL proteins include apoA-II, apoE, apoA-IV, apoCs, apoD, apoH, apoJ, apoL-1, apoM and apoO. One of the major HDL-associated enzymes is lecithin–cholesterol acyltransferase (LCAT). It catalyzes cholesterol esterification to cholesterol esters. HDL is associated with about 75% of plasma LCAT activity.[68] Not at least, HDL functions as one of the major cholesterol carriers in the human blood.[69] Earlier studies suggested that high HDL-C levels decrease the risk of AD, while lower HDL-C levels may correlate with the severity of AD.[70–73]

1.2.2. Apolipoprotein A-I

As mentioned above, apoA-I was identified as the major HDL protein. Important functions of apoA-I involve activation of LCAT, interaction with cellular receptors and motion between other lipoprotein molecules.[68] To generate nascent HDL apoA-I first reacts specifically with ABCA1 and in the next step with LCAT, where nascent HDL is enriched with esterified cholesterol and, thus, forms mature HDL.[74] There is evidence that apoA-I has influence on the pathogenesis and increases the risk of AD by modulating brain cholesterol metabolism.[75,76] Khalil *et al.* proposed that aging modified the apoA-I / ABCA1 dependent cholesterol efflux pathway, probably due to oxidative modifications during aging.[77]

1.2.3. Functions of HDL and apoA-I at the BBB

The existence of the BBB was originally observed by Paul Ehrlich in 1885, when he noted that after injecting water-soluble dye into the circulation brain and spinal cord were the only parts of the body remaining unstained.[78] Later studies discovered its function as a highly specialized structural and biochemical barrier between circulating blood and underlying brain tissues.[79–81] The barrier is formed of a complex network of brain capillary endothelial cells, pericytes and astrocyte foot, being in connection via junctions (Figure 3, adapted from Gerstner *et al.*).[82] Between the endothelial cells, tight junctions control paracellular diffusion of water-soluble substances through the BBB, consisting of transmembrane proteins and cytoplasmic plaque proteins. These junctions raise the endothelial electrical resistance up to 1,500 - 2,000 $\Omega \bullet cm^2$, compared to 3 - 33 $\Omega \bullet cm^2$ in other tissues.[83]

Earlier studies in our lab have revealed that pBCEC are able to produce and secrete apoA-I. Using our 3D-BBB *in vitro* model, a dose- and time-dependent transcytosis of apoA-I across a monolayer of pBCEC was observed in both directions. Moreover, there is evidence that HDL_3 supports the transport of apoA-I.[84] As mentioned above, an upregulation of apoA-I levels and secretion, respectively, due to LXR activation, in combination with increased ABCA1 levels results in formation of HDL-like particles at the brain parenchymal side of the BBB.[42] Our previous results also already showed a decrease in Aβ oligomer levels when treating pBCEC with HDL_3.[85] There is evidence that HDL acts as a repressor of Aβ production via activation of the ABC transporters.[86] Also, HDL can directly bind Aβ, thus, inhibiting its oligomerization and acting as a transporter.[87,88] Finally, results obtained in our lab have implicated that apoA-I enhances the production of sAPPα,[84] the beneficial cleavage product from APP processing.

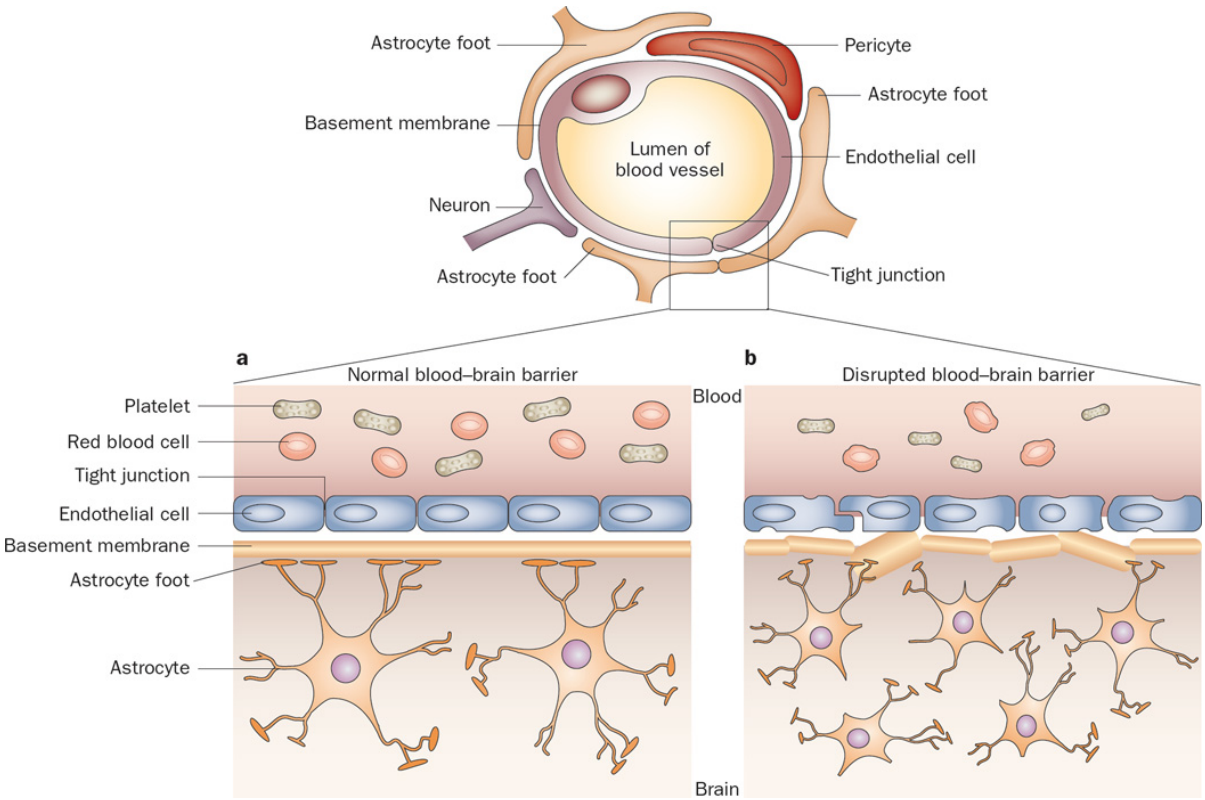

Figure 3: Schematic representation of the BBB. Blood vessels are surrounded by endothelial cells, which are connected via tight junctions. Pericytes, astrocytes and neurons adjoin to the endothelial cells. An intact BBB allows only certain proteins and transporter to move from blood to brain parenchymal compartment and vice versa, whereas a disrupted BBB loses its barrier function. (Figure adapted from Gerstner *et al.* [82])

1.3. Aim of Thesis

The aim of the present thesis was to investigate the effects of both, HDL_3 and apoA-I on Aβ production and clearance in cells constituting the BBB, in particular in brain capillary endothelial cells (BCEC).

Hence, APP and Aβ oligomer levels as well as levels of secretases responsible for specific pathways in APP processing were examined.

Furthermore, using a polarized *in vitro* model mimicking brain and blood sides at the BBB, transport studies of Aβ were performed in the absence or presence of apoA-I or HDL_3. Previous research led to hypothesize that the transporters ABCA1, ABCG1, and LRP1 have supporting roles in the clearance of Aβ across the BBB,[40,41,86,89–92] thus, effects on mRNA and protein levels of these transporters were examined.

Also, we were trying to outline how HDL_3 and apoA-I, respectively, modulate the uptake of Aβ by pBCEC and if they had an impact on cellular ROS production. Most of these experiments were additionally performed in presence of Aβ to mimic AD conditions. Since protein and lipid metabolism of pigs are comparable to humans,[93] BCEC were isolated and cultivated from porcine brains and used for our *in vitro* model.

2. Materials

75 cm^2 cell culture flasks, 6- and 12-well plates were purchased from Greiner Bio-One, Transwell® 12-well plates were obtained from Corning Life Sciences.

2.1. Isolating, Culturing and Treating Cells

Recipes for solutions and medium used during cell isolation, culturing and treating cells are listed below. Reagents purchased are illustrated in Table 1.

1x PBS, 5 Liters

- 40 g NaCl
- 10 g Glucose
- 1.5 g KCl
- 0.457 g NA_2HPO_4 • 2 H_2O
- 0.1 g KH_2PO_4

Fill up to 5 liters with d_2H_2O, stir for 15 min and sterile-filter the solution. The pH should be between 7.38 and 7.42. Store at 4°C.

Dextran Solution

- 163.3 g Dextran
- 2 g $NaHCO_3$
- 91 ml MEM Earle's Medium (10x)

Fill up to 900 ml with d_2H_2O, stir overnight at 4°C, determine and adjust density with d_2H_2O to 1.0612 g/L. Autoclave solution and store at 4°C.

Preparation Medium

- 500 ml Earle's Medium M199 (1x)
- 1% Penicillin / Streptomycin
- 1% Gentamycin
- 1 mM L-Glutamine

Plating Medium A

- 500 ml Earle's Medium M199 (1x)
- 10% Horse Serum
- 1% Penicillin / Streptomycin
- 1% Gentamycin
- 1 mM L-Glutamine

Plating Medium B

- 500 ml Earle's Medium M199 (1x)
- 10% Horse Serum
- 1% Penicillin / Streptomycin
- 1 mM L-Glutamine

Serum Free Medium

- 500 ml Earle's Medium M199 (1x)
- 1% Penicillin / Streptomycin
- 1 mM L-Glutamine

DMEM / Ham's F12 Medium

- 500 ml Dulbecco's Modified Eagle's Medium / Ham's Nutrient Mixture F12
- 1% Penicillin / Streptomycin
- 0.7 mM L-Glutamine
- 0.4% Hydrocortisone stock solution [50 µg/ml]

Collagenase / Dispase Solution

Sterile-filter 140 mg Collagenase / Dispase and 10 ml Plating Medium A and store aliquots at -20 °C.

Percoll® Biphase

1.03 g/ml density

- 40 ml PBS (1x)
- 9 ml Percoll® (pH 8.5 – 9.5)
- 1 ml MEM Earle's Medium (10x)

1.07 g/ml density

- 20 ml PBS (1x)
- 27 ml Percoll® (pH 8.5 – 9.5)
- 3 ml MEM Earle's Medium (10x)

Store at 4°C.

Collagen G Solution [60 µg/ml and 120 µg/ml]

Mix 450 µl [for 60 µg/ml] or 900 µl [for 120 µg/ml] of Collagen G stock solution [4 mg/ml] with 30 ml PBS (1x). Store at 4°C.

Apolipoprotein A-I

Apolipoprotein A-I (apoA-I) is isolated, cleaned up and provided by the working group of ao.Univ.-Prof. Dr.phil. Gernot Desoye, Department of Obstetrics and Gynecology at the Medical University of Graz. Dissolve 1 mg of apoA-I gently in 1 ml PBS. Avoid air bubbles that lead to oxidation. Store aliquots at -20°C.

HDL_3

HDL_3 is isolated and stored as described in “3.2. Isolation”.

Hydrocortisone Stock Solution [50 µg/ml]

Dissolve 1 mg hydrocortisone in 1 ml ethanol and 19 ml DMEM / Ham’s F12 Medium. Store aliquots at -20°C.

Amyloid-beta 1-40 Stock [1 mg/ml]

Dissolve 1 mg amyloid-beta 1-40 ($A\beta_{1-40}$) powder (Sigma Aldrich) in 1 ml PBS and store aliquots at -20°C.

Fluorescent Amyloid-beta 1-40

Incubate 100 µl of amyloid-beta 1-40 [1 mg/ml] with 3 µl Alexa Fluor 488 5-TFP for 1 h at 37°C in 18 µl carbonate bicarbonate (CBC) buffer. Remove unbound fluorescent dye via size-exclusion on a PD-10 column. For elution use 1 ml PBS buffer.

Purchased solutions and chemicals are listed below.

Table 1: Solutions and Chemicals used for Cell Culture Experiments

Product	Company
Amyloid-beta Protein Fragment 1-40	Sigma-Aldrich
Collagen G from bovine calf skin	M&B Stricker
Collagenase / Dispase	Roche
D(+)-Glucose monohydrate	Carl Roth GmbH
Dextran	VWR
Dispase	Life technologies
DMEM / Ham's F12 Medium	Life technologies
Horse Serum	PAA Laboratories
Hydrocortisone	Sigma-Aldrich
L-Glutamine	PAA Laboratories
Earl's Medium 199 (1x)	Life technologies
Minimum Essential Medium (MEM, 10x)	Life technologies
Penicillin / Streptomycin / Gentamycin	PAA Laboratories
Percoll® pH 8.5- 9.5	Sigma-Aldrich
Trypsin- EDTA	PAA Laboratories

2.2. Protein Isolation, SDS-PAGE and Immunoblotting

Chemicals used for protein isolation, SDS-PAGE and immunoblotting are listed in Table 2, antibodies in Table 3. Solutions were prepared as followed:

Protein Lysis Buffer

- 50 mM Tris (pH 7.5)
- 10 mM EDTA
- 1% Triton-X 100
- 1 tablet of protease inhibitor cocktail

Fill up to 10 ml with d_2H_2O. Aliquots are stored at -20°C

Running Buffer (10x)

- 30.3 g Tris
- 144 g Glycin
- 10 g SDS

pH should be set to 8.3.

Transfer Buffer (1x)

- 240 ml Running Buffer (10x)
- 480 ml Methanol

Fill up to 2.4 liters with d_2H_2O and store at 4°C.

TBS-T (1x)

- 100 ml Tris, 1 M, pH 7.5
- 250 ml NaCl, 5 M
- 2.5 ml TWEEN 20

Fill up to 5 liters with d_2H_2O.

Blocking Solution

Dissolve 5% non-fat dry milk Blotting-Grade blocker in 1x TBS-T. Prepare freshly or freeze at -20°C.

Table 2: Materials used for Protein Isolation and Western Blot

Product	Company
Blotting-Grade blocker, non-fat dry milk	Biorad
Bovine Serum Albumine, 2 mg/ml	Thermo Scientific
Cell Proliferation Reagent WST-1	Roche
Centrifuge Sigma 3K15 with angle rotor 12154-H	Sigma
Chemicals	Carl Roth or Sigma Aldrich
CL- Xposure Film (12.5 x 17.5 cm)	Thermo Scientific
Clarity Western ECL Substrate	Biorad
Combi- Shaker KL 2	Carl Roth
Concentrator Plus	Eppendorf
ELMA Transsonic 460, ultrasonic unit	Carl Roth
IKA® Model MS1 mini-shaker	Carl Roth
Magnetic stirrer with heating, MR 3001, Heidolph	VWR
Microcentrifuge, Qualitron DW- 41	Carl Roth
NuPage® MES SDS Running Buffer (20x)	Life technologies
NuPage® MOPS SDS Running Buffer (20x)	Life technologies
NuPage® Novex 4-12% Bis- Tris Midi Gel	Life technologies
Pierce® BCA Protein Assay Kit	Thermo Scientific
Protease Inhibitor Cocktail tablets	Sigma Aldrich
PVDF membrane, Hybond-P	GE healthcare
Ratek RSM7, Rotary Suspension Mixer	VWR
Sunrise photometer with Magellan software	Tecan
XT sample buffer (4x)	Biorad
XT sample reducing agent (20x)	Biorad

Table 3: List of Antibodies used for Immunoblots.

Antibody	Working dilution	Company	Protein detected
Primary antibody			
Rabbit anti β-Actin	1:5,000	Sigma Aldrich	β-Actin
Rabbit anti β-Amyloid Precursor Protein; CTF	1:1,500	Sigma Aldrich	APP_{695}, APP_{751} and APP_{770}; C-terminal fragment
A11 rabbit anti-amyloid oligomer (AHB0052)	1:1,500	Life Technologies	Aβ oligomers
Mouse anti-ABCA1 (AB18180)	1:2,000	Abcam	ABCA1
Rabbit anti-ABCG1	1:1,000	Abcam	ABCG1
Secondary antibody			
Goat anti-rabbit IgG-HRP	1:5,000	Santa Cruz Biotechnology	
Goat anti-mouse-HRP	1:5,000	Sigma Aldrich	

2.3. RNA Isolation, cDNA Synthesis and qRT-PCR

Products and reagents used for RNA isolation, cDNA synthesis and quantitative real time PCR are listed in Table 4. Pre-validated primers for qRT-PCR were ordered from Qiagen or self-designed and purchased from Life technologies, given in Table 5.

Table 4: Materials used for RNA Isolation, cDNA Synthesis and qRT-PCR

Product	Company
0.2 ml PCR Tubes	Biorad
2-Log DNA ladder	New England laboratories
Biozym LE Agarose	Biozym
C-1000™ Thermal Cycler	Biorad
Ethidiumbromide [10 mg/ml]	Life technologies
Gel loading Dye, Blue (6x)	New England laboratories
Hard-Shell® Low-Profile Thin-Wall 96-Well Skirted PCR Plates	Biorad
HE 33 Mini Submarine Electrophoresis Unit	Hoefer® Inc.
High Capacity Reverse Transcriptase Kit	Life technologies
Icycler iQ™, Real-time PCR Detection System	Biorad
iQ SYBR® Green Supermix	Biorad
Microseal 'B' Adhesive Seals for PCR plates	Biorad
Molecular Imager ChemiDoc XRS System	Biorad
NanoDrop® ND-1000 UV-Vis Spectophotometer	Peqlab
Nuclease-free water	Carl Roth
ON target plus siRNA, 5 nmol	Dharmacon
OneTouch Filter-tips, 10 µl	Biozym
Power Pac HC, Power Supply	Biorad

PrimeFect™ Diluent	Lonza
PrimeFect™ siRNA Transfection Reagent	Lonza
Taqman Gene Expression Master Mix	Life technologies
TriReagent RT	Molecular Research Center, Inc

Table 5: Primers used for qRT-PCR

Gene	Forward Primer 5'-3' / Reverse Primer 3'-5'	Amplicon length (bp)
ABCA1	GCCATTCTCCGGGCCAAC	252
	GGCTTCACGCCGCTGAT	
ABCG1	GTTCTCCACGTCCAGCTCTC	225
	CAGGGTTCTTCGTCAGCTTC	
ADAM10	AGCAACATCTGGGGACAAAC	219
	CTTCCCTCTGGTTGATTTGC	
APP	CGTGGGAGTTTAGCTGCTTC	122
	TCAAATGCAATCGTGGAAAA	
BACE1	ACAGTGGCACCACCAACCTT	105
	GCCAGAAACCATCAGGGAAC	
HPRT1	AGGACCTCTCGAAGTGTTGG	247
	CAGATGGCCACAGGACTAGA	
LRP1	GCAGATGTATCAACATCAACTGG	98
	GGGTGCTAGAGCAAGAGTGG	

2.4. Diverse Studies

Materials and reagents for ROS studies, cholesterol efflux studies, Aβ uptake studies and Aβ transport studies can be found in Table 6-9.

Table 6: Materials and Reagents used for ROS Studies

Product	Company
H_2DCFDA dye (Light sensitive)	BIOTREND Chemikalien GmbH
Triton X-100	Carl Roth GmbH
Ethanol	Carl Roth GmbH
Black Eppendorf Tubes (1.5 ml)	Carl Roth GmbH

Table 7: Materials and Reagents used for Cholesterol Efflux Studies

Product	**Company**
[^{3}H]-Cholesterol	Perkin Elmer
NaOH (0.3N)	Merck
Qubit protein assay kit	Invitrogen
Ultima Gold Scintillation Cocktail	New England Nuclear

Table 8: Materials and Reagents used for Aβ Uptake

Product	**Company**
Amyloid-beta 1-40	Phoenix Peptides
Alexa Fluor 488 5-TFP	Invitrogen

Table 9: Materials and Reagents used for Aβ Transport

Product	**Company**
[^{125}I]-Amyloid-beta 1-40	Phoenix Peptides
[^{14}C]-Sucrose	Perkin Elmer
Gamma 5500B	Beckman
Ultima Gold Scintillation Cocktail	New England Nuclear

3. Methods

3.1. Isolation and Culture of Primary Porcine Brain Capillary Endothelial Cells

The method was adjusted from Franke *et al*.[94] Therefore, porcine brain halves were obtained from the local slaughterhouse, quickly rinsed with 75% ethanol and transported in jars filled with PBS containing 2% P/S on ice. Three hemispheres were used for one preparation of brain capillary endothelial cells (pBCEC). A sterile glass plate was placed under the hood and the glass containing the brains in cold PBS on ice next to it. Using forceps the meninges and visible blood vessels were removed gently. Capillaries would remain in the tissue. Further, the choroid plexus was removed generously. Subsequently, the hemispheres were cut into smaller pieces using a scalpel and the tissue was minced with a sterile vegetable cutter. The homogenate then was transferred into a 200 or 250 ml sterile screw-cap bottle containing a magnetic stirrer and Earle's Medium M199 1X preparation medium containing penicillin, streptomycin, gentamycin and L-glutamine were added to obtain a total volume of 100 ml. For the first digestion step 0.07g dispase per 100 ml were added and let stir for 1 to 1½ h at 37°C in a water bath. Following this, 150 ml dextran solution were added to the homogenate and well mixed. The suspension then was portioned into 8 centrifuge tubes and centrifuged at 6,800 g for 10 min at 4°C. After centrifugation the supernatant was discarded, the myelin was scraped off the tube sidewalls, and the remaining pellet containing the endothelial cells was dissolved with 2 ml plating medium A each, carefully resuspended and filtered across a nylon mesh (180 µM). To remove the basal lamina of the capillaries, 350 µl collagenase / dispase solution were added to the cells and very gently stirred in a water bath at 37°C for 1 minute. The cell suspension was centrifuged at 110 g for 10 min, the pellet was resuspended in 5 ml pre-warmed plating medium A. The cell suspension was carefully placed on top of a percoll biphase gradient prepared using 20 ml of 1.03 g/ml percoll solution underlaid with 15 ml of 1.07 g/ml percoll solution. Endothelial cells were separated from other cells and myelin by centrifuging at 1,300 g for 10 min at 15 °C, leaving the break off. After centrifugation, pBCEC were visible in the interphase. The cells were carefully collected with a transfer pipette and washed in 30 ml of plating medium A, with a centrifugation step at 110 g for 10 min. Depending on the size of the cell pellet the cells were resuspended in 7 to 10 ml of

plating medium A and cultivated in 7 to 10 collagen-coated 75 cm² flasks. The flasks were pretreated with 5 to 10 ml of collagen [60 µg/ml], which were replaced with 9 ml of plating medium A before adding 1 ml of the pBCEC suspension and shaking the flasks gently to make sure, the cells were spread equally. The cells then were placed in the 37°C incubator. On the following day the medium was changed to plating medium B after two gentle washing steps using pre-warmed PBS.

Cells were split three days after isolation when they have become confluent. Depending on the experiments, 6-well, 12-well or Transwell® 12-well plates were pretreated with 60 µg/ml or 120 µg/ml collagen, respectively. Once cells were washed gently with 10 ml PBS twice, they were rinsed with 2.5 ml of trypsin/EDTA and incubated for 1 to 2 min at 37°C. The culture flasks were removed and struck against the hand with the edges to quickly remove the endothelial cells attached to the plates, leaving residual pericytes behind. To make sure cells got detached from the plates, the plates were examined under the microscope. The addition of 5 ml plating medium B led to inactivation of trypsin/EDTA. The suspension containing the cells was then transferred into a 50 ml falcon tube, centrifuged at 110 g for 5 to 6 min, and the cell pellet was dissolved in the quantity of plating medium B required. To ensure cells spread equally, plates were shaken gently and then incubated at 37°C in humidified air containing 5% CO_2 for two days until they become 90 to 100 % confluent.

3.2. Isolation of HDL_3 and ApoA-I

ApoE-free HDL_3 [1.125 - 1.210 g/ml] was isolated freshly from normolipidemic humans, described by Sattler *et al.*[95] 7 x 9 ml blood were collected in EDTA tubes. The blood was then centrifuged at 1,100 g for 10 min, 15 °C. Meanwhile, 9 ml of 1.063 g/ml KBr solution were added to the centrifuge tubes using a syringe and stored at 4°C. 38 ml of plasma were added slowly to the light sensitive 13.08 g potassium bromide. To dissolve the chemical, the plasma was incubated on a round shaker and gently shaken for 15 min at 4°C. The density of the plasma mix was controlled. 1 ml plasma should weigh 1.242 g, compared to 1 ml Aqua dest. with 1.014 g. 4.6 ml of plasma solution were added slowly to the bottom of each ultracentrifuge tube containing 9 ml of PBS [1.063 g/ml], air bubbles were removed and the centrifuge tubes were sealed carefully. The solutions then were centrifuged

at 694,000 g for 4 h at 15°C in a Beckman coulter, 90Ti Rotor. In the next step, HDL_2 and HDL_3 were collected. The two HDL forms were visible as two yellow layers in the else clear solution. The upper layer, containing HDL_2, was collected primary. Therefore, the centrifuge tube was poked with a 10 ml syringe and filled with 8 to 9 ml HDL_2 and the syringe was left in the tube. The same procedure was repeated for the yellow layer below, containing HDL_3. To prevent HLD oxidation air bubbles in the syringe were removed. Before using HDL_3, the lipoprotein was desalted using a PD10 “desalting column” and PBS (10 mM, pH 7.4). The concentration of HDL_3 protein was determined with the BCA assay. To prevent oxidation of HDL, argon was filled into the falcon tube to replace oxygen.

ApoA-I was purified after delipidation of HDL by size exclusion chromatography on a Sephacryl S-200 column (3 x 150 cm) as described by Kratzer *et al*.[96]

3.3. BCA Protein Assay

For various experiments the Pierce™ BCA Protein Assay Kit from Thermo Fisher Scientific was used to determine protein concentrations. Solutions A and B were mixed with a ratio of 50:1. Further, 100 µl of the mix were added per well into 96-well microtiter plates and incubated with 4 µl of the protein samples. The plates were incubated in the water bath for 30 min at 37°C, shaking slightly. The kit also provided an albumin standard with a concentration of 2 mg/ml. Multiple dilutions were prepared to generate standard curves. The protein indicator changed from blue to purple after incubation at 37°C and the plates were measured at a wavelength of 562 nm on Sunrise™Tecan plate reader.

3.4. Protein Isolation, SDS-PAGE and Western Blot Analysis

Cells cultured in 6-well plates were incubated with 1 ml serum-free medium plus 20 µg/ml apoA-I or 50 µg/ml HDL_3 in combination with or without 0.5 µg/ml $A\beta_{1\text{-}40}$. As vehicle control PBS was used. After 24 h of treatment the plates were placed on ice, supernatants (media) were collected and cells were rinsed with cold PBS twice.

To isolate cellular proteins, 40 µl of protein lysis buffer were added per well. The cells were scraped off, the suspension was transferred into 1.5 ml Eppendorf tubes, and

vortexed for 30 seconds, followed by 2 times 3 min of sonication in a water bath sonicator with a break of 1 minute in between. The lysates were centrifuged at 10,000 g for 10 min at 4°C to get rid of DNA. After determining the protein concentration with a BCA protein assay cell lysates were stored at -20°C.

To isolate extracellular proteins cell culture supernatants/media were centrifuged at 10,000 g and 4°C for 10 min to remove cellular debris first. Then 100 µl of ice-cold 30% TCA were added per 1 ml medium and vortexed well. Afterwards, the samples were left on ice for 30 min to provide precipitation of proteins. The samples were centrifuged at 10,000 g and 4°C for 10 min, the supernatant was discarded, and the protein pellet washed with 0.5 µl of acetone twice, vortexed, and centrifuged. For the final step the pellet containing the proteins was air-dried and then dissolved in 20 µl 1 x loading buffer.

To detect intra- and extracellular proteins, SDS-PAGE was performed using NuPage® Novex 4-12% Bis-Tris Midi Gels (Thermo Scientific). Protein samples were denaturated at 95°C for 5 min before loaded onto the gels. Proteins were separated by molecular weight using the SDS-PAGE method described by Laemmli.[97] Therefore, gels were run at 180 mV for ~45 min. For immunoblotting (western blotting), separated proteins were blotted onto a 0.45 µm PVDF membrane (GE healthcare) at 50 mV for 1½ h at low temperature. After blocking with 5% skim milk powder for 1 h, the membrane was washed with TBS-T for 7 min and incubated with a primary antibody at 4°C over night. On the following day, the membrane was washed three times for 7 min using TBS-T, and incubated with secondary HRP-conjugated goat anti-rabbit antibody for 1½ h. After another 3 x 7 min of washing with TBS-T, the membrane was incubated with ECL substrate (Biorad) for 2-5 min and immunoreactive bands were detected using the ChemiDoc™ Touch Gel Imaging System (Biorad). Image Lab software (Biorad) was used for densitometry. List of antibodies used see page 17, Table 3: List of Antibodies used for Immunoblots.

3.5. RNA Isolation and qPCR

After culturing and incubating pBCEC in 6-well plates, the medium was removed and 330 µl TRI ReagentRT were added onto the cells. Samples of three wells were pooled in Eppendorf tubes and 50 µl BAN were added. The mixture then was inverted for over 20 times and incubated at room temperature for 5 min. The suspension was centrifuged at 12,000 g for 15 min at 4°C. The resulting aqueous phase was transferred into fresh Eppendorf tubes and RNA precipitated by adding 500 µl isopropanol. The samples were left at room temperature for 10 min and then centrifuged at 12,000 g and 4°C for another 8 min. The RNA appeared as a white pellet and was washed with 1 ml 75% ethanol, centrifuged at 7,500 g and 4°C for 5 min. Once the supernatant was removed, the pellet was air-dried until the ethanol evaporated completely. Depending on the size of the pellet 50 to 100 µl RNAse free water was added and incubated at 55-60°C for 10 to 15 min at 300 rpm. Finally, the RNA content was measured using a NanoDrop 1,000. To transcribe RNA into cDNA, High Capacity Reverse Transcriptase Kit (Life technologies) was used. The resulting cDNA was diluted to an end-concentration of 2.5 ng/µl. For qPCR 5 µl SYBR green, 0.3 µl forward and reverse primer as well as 2.4 µl nuclease free water were used per 2 µl (= 5 ng) RNA. Relative gene expression was quantified by setting the housekeeping gene HPRT1 as reference and the *ΔΔCt* method described by Livak and Schmittgen.[98] List of primers used see page 18, Table 5: Primers used for qRT-PCR.

3.6. Reactive Oxygen Species (ROS) Assay

The pBCEC were cultured in 12-well plates. After incubation with 500 µl of serum-free medium with either 2 or 20 µg/ml apoA-I or 20 µg/ml or 50 µg/ml HDL_3, respectively, each of the 4 treatments in the absence or presence of 0.5 µg/ml $A\beta_{1-40}$ for 24 h, cells were washed with pre-warmed PBS. Addition of 600 µl pre-warmed 10 µM light sensitive H_2DCFDA/PBS solution for 20 min at 37 °C led to fluorescent staining of ROS. Subsequently, cells were washed with ice cold PBS and lysed in 300 µl 3% Triton X-100 in PBS for another 30 min at 4°C. To improve the solubilisation of the fluorescent dye, 50 µl of absolute ethanol were added and shaken for additional 15 min before transferring the lysates into black Eppendorf tubes and centrifuging at 10,000 g for 10 min at 4°C to remove cellular debris. 100 µl

of the supernatant were pipetted into 96-well microtiter plates in duplicates. The fluorescence was measured at excitation and emission wavelength of 485 and 530 nm, respectively. To determine cell protein content, a BCA protein assay was performed and fluorescence was normalized to the protein concentration.

3.7. Cholesterol Efflux

Cells were cultured in 12-well plates for two days before incubation with 500 µl Plating medium B including 0.5 µCi/ml [^{3}H]-cholesterol at 37°C in humidified air containing 5% CO_2. 24 hours later, cells were washed with pre-warmed PBS twice and incubated for 4 h in 1 ml pre-warmed serum-free medium per well for equilibration of cellular cholesterol pools. Cells were then washed twice and incubated with 20 µg/ml apoA-I or 50 µg/ml HDL_3 in the absence and presence of 0.5 µg/ml $A\beta_{1\text{-}40}$, respectively, whereby 1 ml of serum-free medium was added per well. Time points of 2, 4, and 24 h, 200 µl of the media were collected and transferred to 5 ml scintillation cocktail (New England Nuclear). The amount of [^{3}H]-labeled cholesterol effluxed from the cells to the medium was determined by beta counting. At 24 h, the remaining medium was discharged, the cells were washed with PBS twice and 300 µl of 0.3 N NaOH were added to each well. The plates were incubated at 4°C over night to assure lysis of the cells. The plates then were put on a shaker at room temperature for 15 to 20 min before beta counting 200 µl of the lysates. To determine the protein content, 10 µl of the lysate were measured using the Qubit protein assay kit and fluorimeter from Thermo Fisher Scientific. Finally, values obtained from media were normalized to the protein content and the amount of [³H]-cholesterol in the lysates. Cholesterol efflux was calculated as the percentage of the sum of the total medium and cellular counts/min.

3.8. Aβ Uptake

To quantify uptake of $A\beta_{1\text{-}40}$ by pBCEC, the cells were cultured in 12-well plates. When grown confluent pBCEC were incubated for 24 h with 500 µl of serum-free medium containing 2 or 20 µg/ml apoA-I or 20 µg/ml or 50 µg/ml HDL_3, respectively. Subsequently, 0.5 µg/ml of fluorescent-labeled (Alexa Fluor 488)-$A\beta_{1\text{-}40}$ in serum free medium were added and cells were incubated for another 2 h at 37°C. From each

well 3 x 100 µl medium were pipetted into black 96-well microtiter plates with clear bottom and the fluorescence was measured at a wavelength of 490-525 nm. pBCEC were washed with PBS twice, 200 µl of 0.3 N NaOH were added to the cells and the plates were stored at 4°C over night to lyse the cells properly before determining the protein concentration with the BCA protein assay. The results obtained were presented in relative fluorescence units (RFU)/100 mg protein.

3.9. Aβ Transport Study across polarized pBCEC

To establish polarized pBCEC cultures, cells were plated onto collagen-coated [120 g/ml] Transwell® (12-well) culture dishes at a density of 40,000 cells/cm^2. Cells were grown for 2–3 days depending on the transendothelial electrical resistance (TEER; 50 Ω•cm^2). The tightness of the Transwell® culture was assessed by measuring the TEER using an EndOhm tissue resistance measurement chamber and EndOhm ohmmeter (World Precision Instruments). TEERs of collagen-coated, cell-free filters were used as blanks. Tight junction formation was induced (overnight) by adding DMEM/Ham's F-12 medium containing 550 nM hydrocortisone along with the treatments indicated below. Establishment of intact tight junctions was indicated by TEERs rising between 100 and 1,000 Ω•cm^2 in the *in vitro* BBB model system. 1.2 ml of medium were added to the basolateral (lower) chamber and 0.5 ml were added to the apical (upper) chamber of the Transwell®system. The cells were incubated at 37°C for 2 hours before removing the medium from the basolateral chamber and 1.2 ml of DMEM Hams hydrocortisone including treatment together with [^{125}I]-$A\beta_{1-40}$ and [^{14}C]-sucrose, used as control for paracellular transport, were added and incubated for another 2 h. 10% of the volume from the apical or basolateral side were mixed with 5 ml scintillation cocktail (New England Nuclear) and measured in the beta counter. Meanwhile, 80% from the remaining apical as well as from the basolateral media were transferred into gamma counter tubes and set on ice. 30% TCA was added in an amount equal to 10% of the sample volume. After vortexing, the samples were left on ice for additional 30 min before the tubes were centrifuged at maximal speed for 10 min at 4°C. The supernatant was transferred into new tubes and measured in the gamma counter. The beta counts are indicators for cell density and quality of the tight junctions formed due to the addition of hydrocortisone to the medium. The ratio of gamma to beta counts was calculated and represents the

intensity of [^{125}I]-Aβ_{1-40} transport from the basolateral side simulating the brain parenchymal side to the apical side simulating the blood side. The transcytosis quotient (TQ) was calculated as followed:

$$A\beta\ TQ = \frac{\frac{[^{125}I] - A\beta\ acceptor}{[^{125}I] - A\beta\ input}}{\frac{[^{14}C] - sucrose\ acceptor}{[^{14}C] - sucrose\ input}}$$

3.10. Analysis and Statistics

Results obtained are presented as mean±SEM. All experiments were performed three times unless stated otherwise. Statistical significances (*p≤0.05; **p≤0.01; ***p≤0.001) were determined by two-tailed Student's *t* test or analysis of variance (ANOVA), performed by using Prism software (*Graphpad* version 6, CA, USA). Intensity levels of western blot protein band signals were analyzed with Image Lab software (*Bio-Rad Labs* version 5).

4. Results

4.1. HDL_3 and HDL_3 in Combination with $A\beta_{1-40}$ increase extracellular Amyloid-beta Oligomer Levels

Prior studies from our group suggest that HDL_3 has the ability to decrease Aβ oligomer levels in pBCEC,[85] while apoA-I increases sAPPα levels in pBCEC.[84] To further gain insights into the effects of HDL_3 and apoA-I on APP, the precursor protein of both, sAPPα and Aβ, primary pBCEC were treated with vehicle control (PBS), apoA-I [20 µg/ml], or HDL_3 [50 µg/ml], respectively, all three in the absence or presence of $A\beta_{1-40}$ [0.5 µg/ml] for 24 h.

To measure mRNA levels, RNA was isolated from the cells, transcribed into cDNA and qRT-PCR was performed using the housekeeping gene HPRT1 as reference. Data were analyzed using the *ΔΔCt* method. To investigate APP protein levels, cellular proteins were isolated and immunoblots with specific full-length APP antibodies (listed in Table 3) performed yielding a signal detected at ~110 kDa (Figure 4 C). Interestingly, although no increase was observed in APP mRNA levels (Figure 4 A), protein levels of APP increased with PBS plus Aβ and with HDL_3 with or without Aβ, as compared to control conditions (Figure 4 B). The addition of 0.5 µg/ml $A\beta_{1-40}$ to the vehicle control increased APP protein levels by 2.4-fold. An even higher impact was observed with HDL_3 (3.8-fold) or HDL_3 in combination with $A\beta_{1-40}$ (4.4-fold) compared to vehicle control.

Subsequently, the question was addressed how Aβ oligomer levels were affected with the conditions mentioned above. Analyzing intracellular Aβ oligomer protein levels using a specific Aβ oligomer antibody (listed in Table 3) yielded bands detected at ~16 kDa (tetramers) and ~36 kDa (octamers) (Figure 5 C). Prior studies from our group suggested that 50 µg/ml HDL_3 reduces Aβ oligomer levels in pBCEC.[85] Contrary to expectations, the present results revealed no significant changes between the treatments. Interestingly, extracellular oligomer levels found in pBCEC supernatants were only detected in a much higher molecular mass range at ~220 kDa (Figure 5 C) and increased by 2.4-fold with HDL_3 and 3.6-fold with HDL_3 in combination with $A\beta_{1-40}$ (Figure 5 B). Although more thorough analysis is required, at present these findings may suggest that HDL_3 binds Aβ oligomers and perhaps transports them from the cell to the environment / medium.

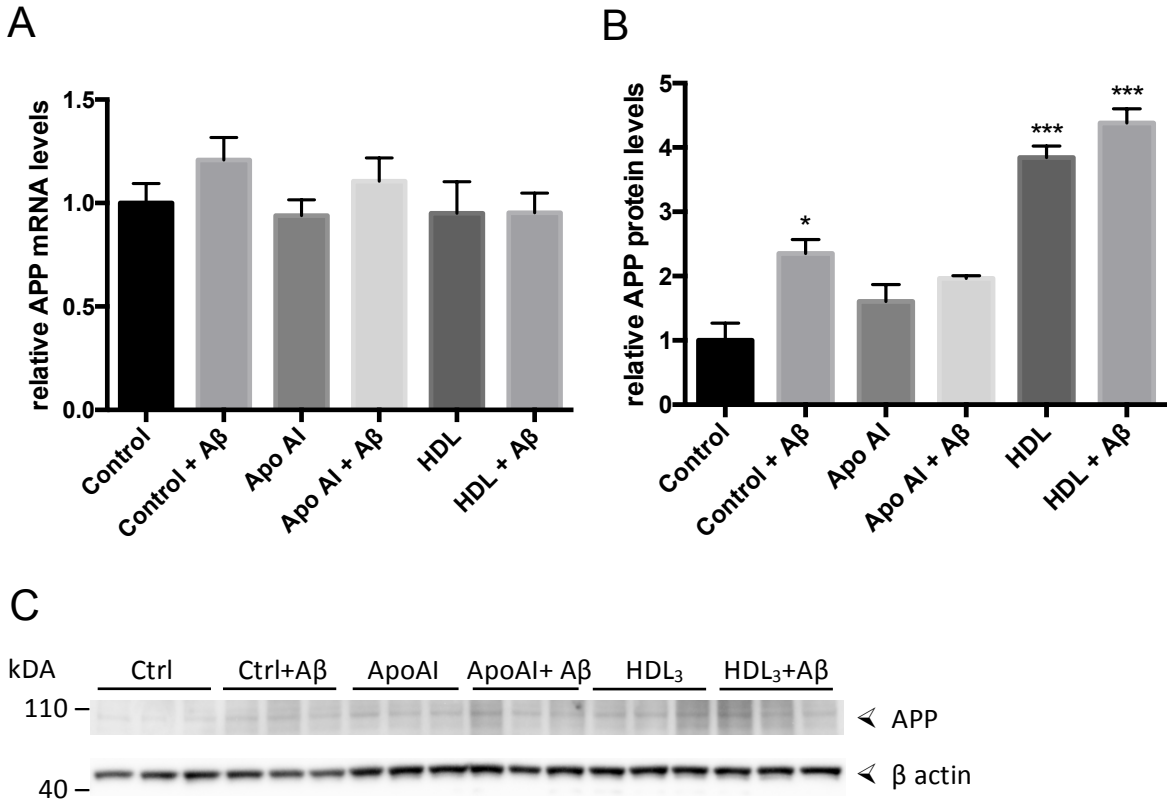

Figure 4: HDL_3 increases APP levels in pBCEC. Cells were incubated with vehicle control (PBS), vehicle control + $A\beta_{1\text{-}40}$ [0.5 µg/ml], apoA-I [20 µg/ml], apoA-I [20 µg/ml] + $A\beta_{1\text{-}40}$ [0.5 µg/ml], HDL_3 [50 µg/ml] as well as HDL_3 [50 µg/ml] + $A\beta_{1\text{-}40}$ [0.5 µg/ml] for 24 h in serum free conditions. mRNA levels of APP (A) were analyzed using qRT-PCR method and normalized to the housekeeping gene HPRT1. Aβ precursor protein (APP) protein levels were detected via western blot and normalized to β actin (B+C). mRNA data represent mean±SEM from 3, protein data from 2 independent experiments performed in triplicates. *p≤0.05; **p≤0.01; ***p≤0.001 versus control.

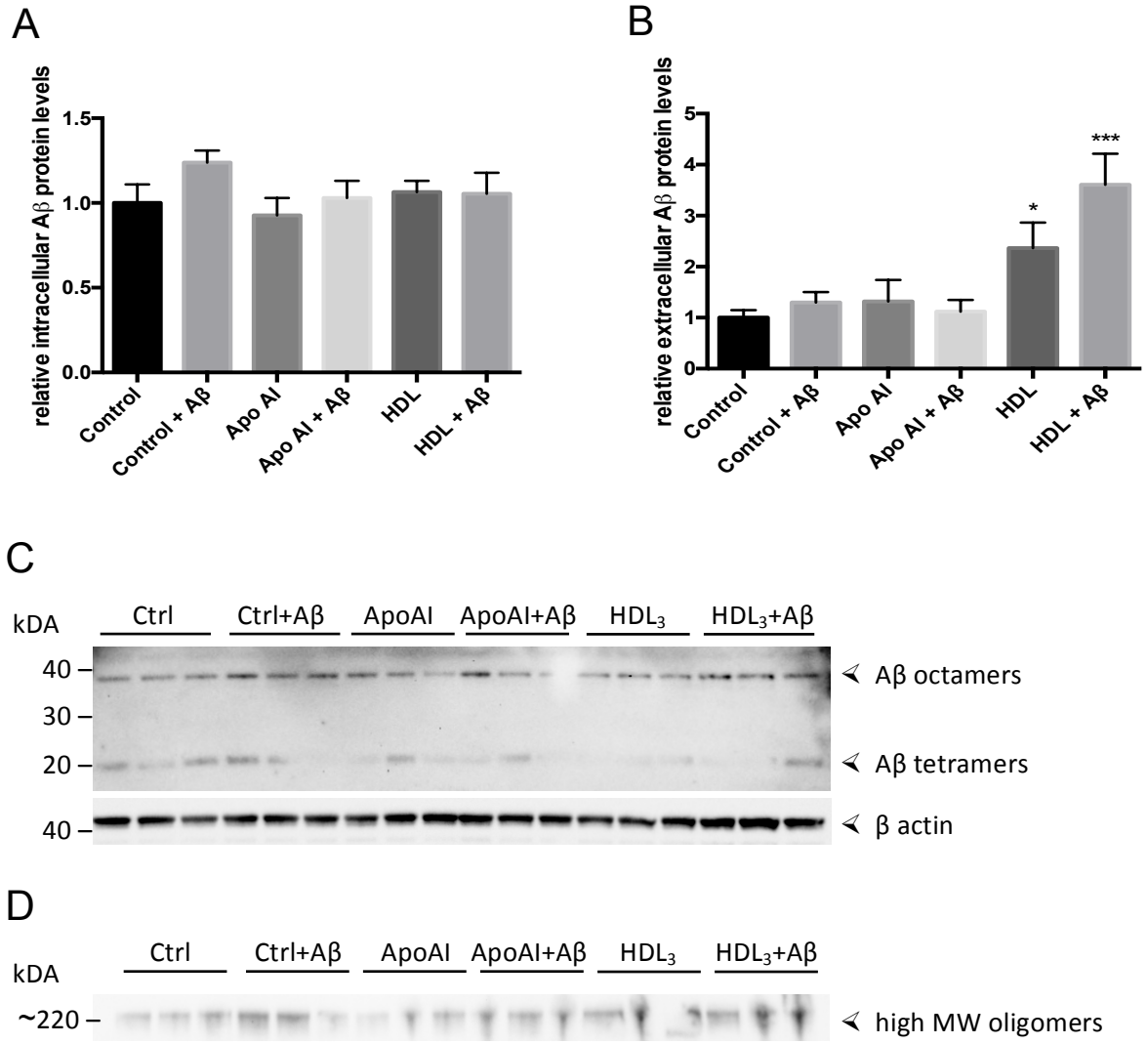

Figure 5: HDL_3 and HDL_3 + $Aβ_{1-40}$ lead to higher extracellular amyloid-beta oligomer levels. Cells were incubated with vehicle control (PBS), vehicle control + $Aβ_{1-40}$ [0.5 µg/ml], apoA-I [20 µg/ml], apoA-I [20 µg/ml] in combination with $Aβ_{1-40}$ [0.5 µg/ml], HDL_3 [50 µg/ml] and HDL_3 [50 µg/ml] in combination with $Aβ_{1-40}$ [0.5 µg/ml] for 24 h in serum free medium. Intracellular (A) and extracellular (B) Aβ oligomer levels were detected via western blot analysis. Triplicates were performed. Densitometric evaluation was performed using Image Lab software (Bio-Rad Labs version 5) and results show mean±SEM from 3 independent experiments. *p≤0.05; **p≤0.01; ***p≤0.001 versus control. Representative western blot images of intracellular Aβ oligomers show no differences (C) but there is an increase in extracellular high-molecular mass oligomer levels (D).

4.2. Transcription of ADAM10 and BACE1 is not altered by Treatment with $A\beta_{1-40}$, apoA-I or HDL_3

Changes in APP protein levels in preceding experiments raised the question whether HDL_3 and/or HDL_3 in combination with Aβ modulate the amount of α-secretase ADAM10 and β-secretase BACE1 and, thus, influence the processing of APP. pBCEC were incubated with vehicle control (PBS), apoA-I [20 µg/ml] or HDL_3 [50 µg/ml], in absence or presence of $A\beta_{1-40}$ [0.5 µg/ml] in serum free medium for 24 h before RNA was isolated and transcribed into cDNA. qRT-PCR was performed and analyzed with the *ΔΔCt* method. Neither for ADAM10 (Figure 6 A) nor for BACE1 (Figure 6 B) significant changes in mRNA levels between the different concentrations were recorded. It is important to note, however, that these results are no stringent prove that protein levels of the secretases are not affected, nor can we tell whether and how the activity of the two enzymes is modulated.

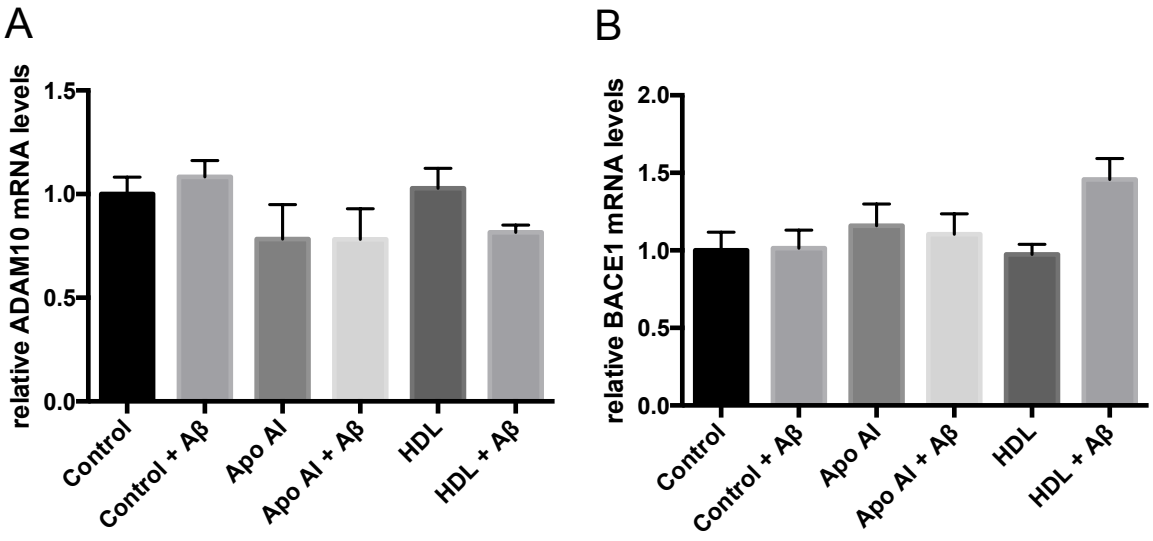

Figure 6: mRNA levels of ADAM10 and BACE1 are not significantly altered after treatment with $A\beta_{1-40}$, apoA-I or HDL_3. Cells were incubated with vehicle control (PBS), vehicle control + $A\beta_{1-40}$ [0.5 µg/ml], apoA-I [20 µg/ml], apoA-I [20 µg/ml] + $A\beta_{1-40}$ [0.5 µg/ml], HDL_3 [50 µg/ml] and HDL_3 [50 µg/ml] + $A\beta_{1-40}$ [0.5 µg/ml], respectively, for 24 h in serum free conditions. mRNA levels of ADAM10 (A) and BACE1 (B) were evaluated via qRT-PCR and normalized to the housekeeping gene HPRT1. Data summarize mean±SEM from 3 independent experiments performed in triplicates. *p≤0.05; **p≤0.01; ***p≤0.001 versus control.

4.3. ApoA-I and HDL_3 prevent Reactive Oxygen Species (ROS) Production in pBCEC

ROS have been noticed to be an important factor in the pathogenesis of AD. In the past, accumulation of Aβ peptides was consistently associated with increased ROS levels and Aβ was proven to promote formation of hydrogen peroxides and lipid peroxides.[28–33] To determine potential effects of HDL_3, apoA-I, and $Aβ_{1-40}$ on ROS levels, pBCEC were incubated with vehicle control (PBS) or in the presence of increasing concentrations of apoA-I [2 µg/ml and 20 µg/ml] and HDL_3 [20 µg/ml an 50 µg/ml], respectively, with or without $Aβ_{1-40}$ [0.5 µg/ml]. After 24 h, fluorescence in the cell lysates was measured. The addition of 0.5 µg/ml $Aβ_{1-40}$ had no significant impact on ROS formation. Interestingly, however, as compared to control conditions ROS levels decreased as the concentration of apoA-I (Figure 7 A) or HDL_3 (Figure 7 B) increased. Thus, a significant reduction in ROS levels was exerted by 2 µg apoA-I (only in the presence of Aβ), by 20 µg/ml apoA-I (~11%) and by 50 µg HDL_3 (~24%; regardless if Aβ was present). These results suggest that both apoA-I and HDL_3 may protect pBCEC from production of ROS.

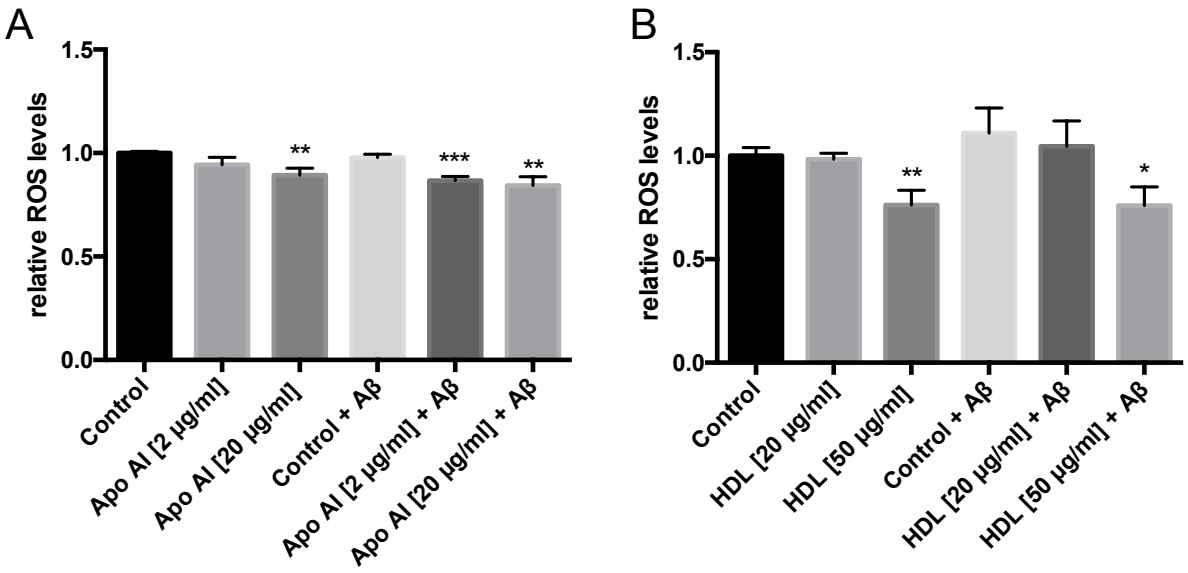

Figure 7: ApoA-I and HDL_3 prevent pBCEC of reactive oxygen species (ROS) production. Cells were treated with two different concentrations [2 µg/ml and 20 µg/ml] of apoA-I in and without the presence of $Aβ_{1-40}$ [0.5 µg/ml] (A) or two different concentrations [20 µg/ml and 50 µg/ml] of HDL_3 with or without $Aβ_{1-40}$ [0.5 µg/ml] (B) for 24 h in serum free medium. ROS were dyed using fluorescent H_2DCFDA dye. Once the cells were lysed, fluorescence was measured and normalized to protein concentrations. Results show mean±SEM from 3 independent experiments performed in triplicates. *p≤0.05; **p≤0.01; ***p≤0.001 versus control.

4.4. Aβ does not compromise Cholesterol Efflux from pBCEC

A major function of both, lipid-free apoA-I and HDL is to serve as acceptors for (excess) cellular cholesterol released from the cell in their presence via ABCA1 and ABCG1 efflux pumps, respectively, pathways, which are also highly active in pBCEC.[42,58] To determine the cholesterol efflux activity of pBCEC when treated with apoA-I, HDL_3 and/or $A\beta_{1-40}$, cells were labeled with [^{3}H]-cholesterol, cellular cholesterol pool equilibrated, and incubated in serum free medium in the absence or presence of apoA-I [20 µg/ml] or HDL_3 [50 µg/ml], with and without $A\beta_{1-40}$ [0.5 µg/ml]. Time dependent cholesterol efflux was measured by counting beta rays in the medium after 2 h, 4 h and 24 h. As expected, apoA-I moderately induced cholesterol release from pBCEC while HDL_3 more efficiently promoted cholesterol release from pBCEC. The presence of 0.5 µg/ml $A\beta_{1-40}$ did not alter cholesterol efflux activity of pBCEC, neither under basal conditions, nor in the presence of cholesterol acceptors apoA-I or HDL_3, suggesting that the ability of pBCEC to release cholesterol is maintained in the presence of [0.5 µg/ml] $A\beta_{1-40}$.

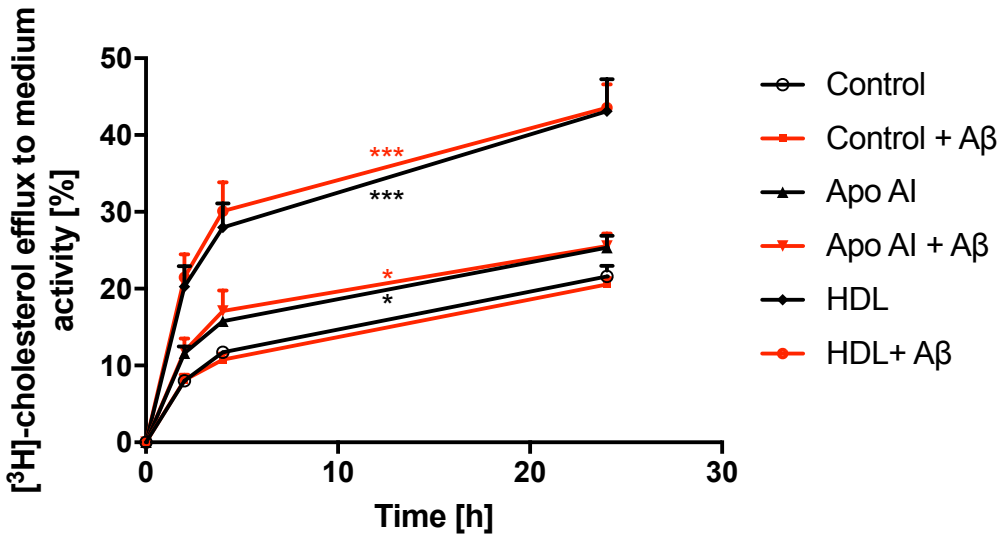

Figure 8: $A\beta_{1-40}$ treatment does not affect apoA-I and HDL-mediated cholesterol efflux activity in pBCEC. Cells were labeled with [^{3}H]-cholesterol for 24 h and equilibrated for 4h. Then they were incubated with vehicle control (PBS), vehicle control + $A\beta_{1-40}$ [0.5 µg/ml], apoA-I [20 µg/ml], apoA-I [20 µg/ml] + $A\beta_{1-40}$ [0.5 µg/ml], HDL_3 [50 µg/ml] or HDL_3 [50 µg/ml] + $A\beta_{1-40}$ [0,5 µg/ml], respectively, for 24 h in serum free medium. Samples were taken after 2 h, 4 h and 24 h and [^{3}H]-labeled cholesterol was measured in the medium during these time points by a beta-counter. The figure illustrates the mean±SEM from 3 independent experiments performed in triplicates. Statistical significances (*p≤ 0.05; **p≤0.01; ***p≤0.001 versus control) were determined by analysis of variance (ANOVA).

4.5. HDL_3 enhances ABCG1 and LRP1 Expression in pBCEC when treated in Combination with $A\beta_{1-40}$

We next examined whether expression levels of ATP-binding cassette transporters (ABC) A1 and ABCG1 correlate with the magnitude of cholesterol efflux activity observed. In addition, mRNA expression levels of lipoprotein related-receptor protein 1 (LRP1) was determined by qRT-PCR. pBCEC were incubated with vehicle control (PBS), apoA-I [20 µg/ml] or HDL_3 [50 µg/ml], respectively, in absence or presence of $A\beta_{1-40}$ [0.5 µg/ml] for 24 h in serum free medium. RNA and proteins were isolated and qRT-PCR/immunoblots were performed. For the ABCA1 immunoblot two bands at ~220 kDa, characteristic for ABCA1, were detected (Figure 9 C) but revealed no significant changes after 3 series of experiments in protein (Figure 9 B) nor mRNA (Figure 9 A) levels after 24 h of incubation with $A\beta_{1-40}$ and/or apoA-I and/or HDL_3.

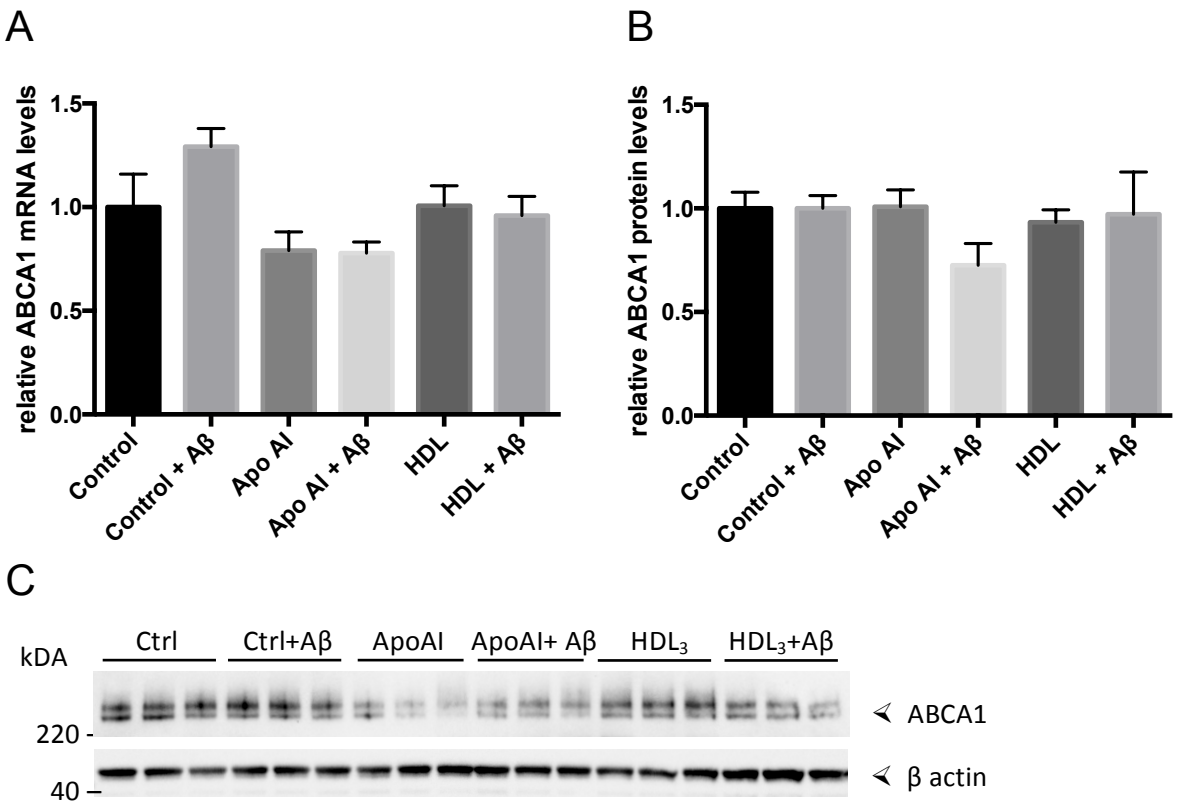

Figure 9: ApoA-I and HDL_3 do not affect ABCA1 protein and mRNA levels. pBCEC were incubated with vehicle control (PBS), vehicle control + $A\beta_{1-40}$ [0.5 µg/ml], apoA-I [20 µg/ml], apoA-I [20 µg/ml] in combination with $A\beta_{1-40}$ [0.5 µg/ml], HDL_3 [50 µg/ml] and HDL_3 [50 µg/ml] in combination with $A\beta_{1-40}$ [0.5 µg/ml] for 24 h in serum free conditions. mRNA levels (A) and protein levels (B + C) of ATP-binding cassette transporter ABCA1 were detected using qRT-PCR / western blot. Statistics represent mean±SEM from 3 independent experiments performed in triplicates. *p≤0.05; **p≤0.01; ***p≤0.001 versus control.

Interestingly, HDL_3 [50 µg/ml] in combination with $A\beta_{1-40}$ [0.5 µg/ml] upregulated mRNA expression of ABCG1 by 2-fold (Figure 10 A).

Regarding expression of LRP1, HDL_3 treatment moderately (1.4-fold) and HDL_3 in combination with $A\beta_{1-40}$ substantially (2.1-fold) increased transcription (Figure 10 B).

These results together led us to believe that higher ABCG1 and LRP1 levels detected in pBCEC after treatment with HDL_3 plus $A\beta_{1-40}$, respectively, may promote the chaperone function of HDL in binding Aβ peptides and/or increased transport of Aβ across the BBB.

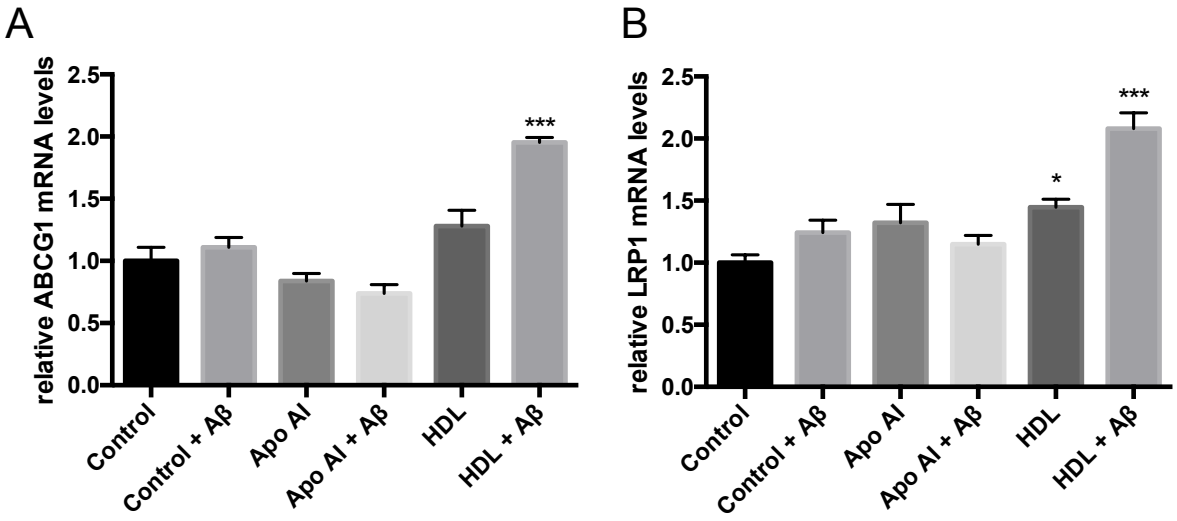

Figure 10: HDL_3 increases ABCG1 and LRP1 expression in combination with $A\beta_{1-40}$. pBCEC were incubated with vehicle control (PBS), vehicle control + $A\beta_{1-40}$ [0.5 µg/ml], apoA-I [20 µg/ml], apoA-I [20 µg/ml] + $A\beta_{1-40}$ [0.5 µg/ml], HDL_3 [50 µg/ml] or HDL_3 [50 µg/ml] + $A\beta_{1-40}$ [0.5 µg/ml] for 24 h in serum free conditions. The mRNA expression levels of ATP-binding cassette sub-family G member 1, ABCG1 (A), and lipoprotein related-receptor protein 1, LRP1 (B), were investigated by using qRT-PCR method. Values were normalized to the housekeeping gene HPRT1. Data show mean±SEM from 3 independent experiments performed in triplicates. *p≤0.05; **p≤0.01; ***p≤0.001 versus control.

4.6. ApoA-I inhibits Uptake of $A\beta_{1-40}$ by pBCEC

To confirm the hypothesis that HDL_3 can bind Aβ and, thus, increases its transport from the brain parenchymal compartment to the blood compartment, transport studies were performed. Therefore, pBCEC were cultured on Transwell® filters to simulate a 3D BBB model. Hydrocortisone was added for 24 h to induce formation of tight junctions. pBCEC further were incubated with apoA-I [2 µg/ml and 20 µg/ml] or HDL_3 [20 µg/ml and 50 µg/ml], respectively, for 24 h. Subsequently, [^{125}I]-labeled $A\beta_{1-40}$ and [^{14}C]-sucrose, used as control for paracellular transport, were added to the basolateral chamber (mimicking the brain parenchymal side) and transport to the apical chamber (mimicking the blood side) was investigated. To determine the amount of [^{125}I]-labeled $A\beta_{1-40}$ transported from basolateral to apical side, gamma counts were measured and normalized to beta counts, detecting [^{14}C]-labeled sucrose. Contrary to expectations, no significant changes were observed after treatment with lower and higher concentrations of apoA-I or HDL_3 (Figure 11 A).

Since the transport studies remained without significant findings, the question raised whether Aβ could be uptaken by pBCEC. For the following Aβ uptake assay the concentrations of apoA-I and of HDL_3 remained the same. After 24 h of incubation with apoA-I or HDL_3 fluorescent-labeled $A\beta_{1-40}$ was added for 2 h and decrease of fluorescence in the medium and, therefore, uptake in the cells was determined by measuring fluorescence present in the medium at a wavelength of 490-525 nm. Interestingly, a lower concentration of apoA-I [2 µg/ml] decreased the uptake of $A\beta_{1-40}$ reduced by over 43%. Higher concentration of apoA-I [20 µg/ml] only led to uptake-reduction of 19%. HDL_3 did not influence the uptake of $A\beta_{1-40}$ in a significant way (Figure 11 B).

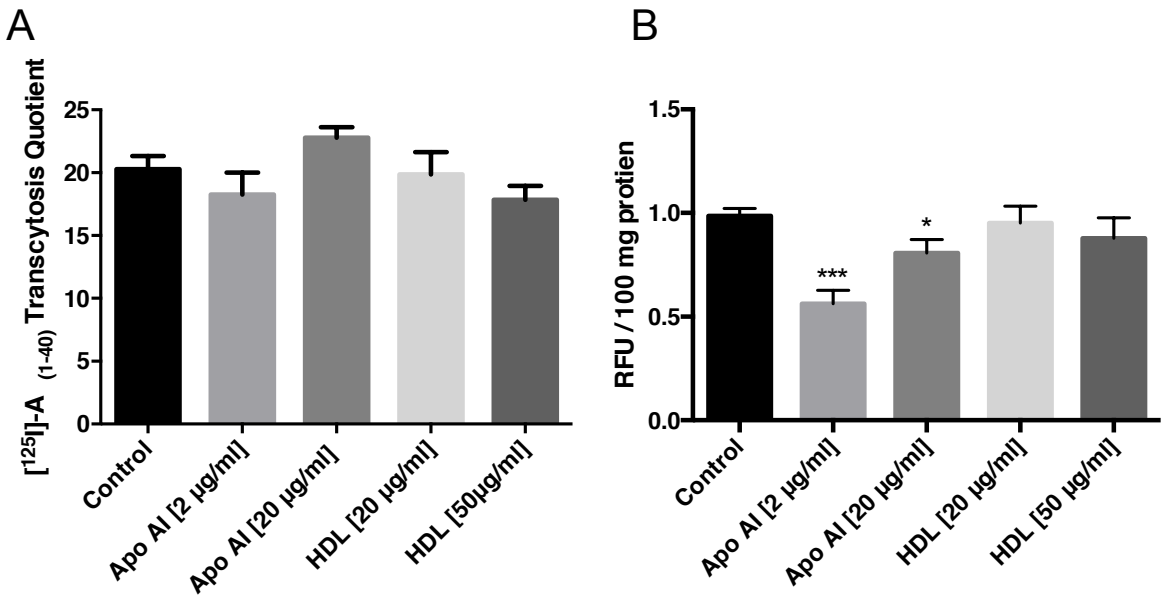

Figure 11: ApoA-I and HDL_3 show no significant changes in transport of $A\beta_{1-40}$ from brain to blood side but apoA-I inhibits uptake of $A\beta_{1-40}$. pBCEC were cultured in Transwells® 12-well to investigate Aβ transport from basolateral (brain) to apical (blood) side. Transendothelial electrical resistance was monitored every day and when reaching >50 Ω•cm^2, cells were incubated with hydrocortisone [550 nM] for 24 h to induce tight junction formation. Then the cells were incubated with apoA-I [2 µg/ml or 20 µg/ml] or HDL_3 [20 µg/ml or 50 µg/ml] in serum free medium for 24 h before medium containing [^{125}I]-labeled $A\beta_{1-40}$ [0.3 nM] and [^{14}C]- sucrose [100 nM], used as control for paracellular transport, was added to the basolateral chamber. [^{125}I]-labeled $A\beta_{1-40}$ was measured in the medium from the apical chamber using a gamma counter. For the Aβ uptake assay (B) cells cultured on 12-well plates were incubated with two concentrations of apoA-I [2 µg/ml and 20 µg/ml] or HDL_3 [20 µg/ml and 50 µg/ml] in serum free medium. After 24 h, fluorescent-labeled (Alexa Fluor 488)$A\beta_{1-40}$ was added for 2 h and decrease of fluorescence in the medium and therefore uptake in the cells was determined measuring the fluorescence at a wavelength of 490-525 nm. Data shown are mean±SEM of 2 independent experiments for the Aβ transport study and 3 independent experiments for the Aβ uptake assay performed in triplicates. *p≤0.05; **p≤0.01; ***p≤0.001 versus control.

5. Discussion

The purpose of the current study was to determine the effects of HDL_3 and apolipoprotein A-I (apoA-I) on amyloid-beta production in primary porcine cerebrovascular endothelial cells (pBCEC) and its transfer at the blood-brain barrier (BBB).

It is understood that amyloid-beta (Aβ) plays a key role in the development and pathogenesis of Alzheimer's disease (AD).[16,99–101] Results obtained in this work show that treatment of pBCEC with Aβ, HDL_3 and a combination of both increase intracellular APP levels. Studies of the two enzymes α-secretase ADAM10 and β-secretase BACE1 revealed no changes in mRNA expression levels leaving space for speculations whether APP gets cleaved into the neuroprotective sAPPα or the toxic Aβ. To answer this question, intra- and extracellular Aβ oligomer levels were investigated via immunoblots using an oligomer antibody (Table 3: List of Antibodies used for Immunoblots.). Prior studies from our group have suggested that HDL_3 reduces Aβ formation *in vitro*.[87] Results presented here failed to show changes with HDL_3 in cellular Aβ oligomer formation, taking into account that the oligomer antibody from the past experiments differs from the one used in the present studies. However, interestingly, HDL_3 led to 2.4-fold increased extracellular Aβ oligomer levels, and even to 3.6-fold increase when cells were treated with HDL_3 combined with Aβ monomers. Remarkably, oligomers found in the medium were detected in a high-molecular mass range. The oligomer-specific antibody A11 used for these studies was already previously recorded to detect a wide variety of amyloidogenic peptides and proteins in a higher-molecular mass range, recognized as pre-fibrillar oligomers.[102] The effects observed with incubation of pBCEC with HDL, may suggest that HDL_3 binds Aβ oligomers and enhances their transport out of the cells. Future studies will aim to clarify whether HDL may prevent further accumulation and formation of fibrils from pre-fibrillar Aβ oligomers.

Our group was able to previously show in pBCEC that both lipid-free apoA-I and HDL_3 function as acceptors for cellular cholesterol.[42,58] In agreement to those prior studies, apoA-I moderately induced cholesterol release from pBCEC, while HDL_3 more efficiently promoted cholesterol release. Therefore efflux pumps ABCA1 and ABCG1 release cholesterol from the cells towards apoA-I and HDL_3, respectively.[42,58,60,103] The presence of 0.5 µg/ml $Aβ_{1-40}$ did not alter cholesterol efflux activity of pBCEC, indicating that BCEC are maintaining cellular cholesterol balance

under simulated conditions of $A\beta_{1-40}$ challenge. Due to these results, we investigated mRNA levels of ABCA1 and ABCG1. In addition to their crucial role in promoting cellular cholesterol efflux, it has been reported that apoA-I and HDL_3 exert anti-inflammatory effects via these cholesterol transporters.[104]

While most studies focus on ABCA1 and its clearance effect on Aβ depositions, [86,89–92] in these studies, using pBCEC, ABCA1 was affected by neither $A\beta_{1-40}$, apoA-I, nor HDL_3.

Surprisingly, however, we found a significant increase in ABCG1 mRNA levels, despite unchanged cholesterol efflux to HDL_3 observed, with the treatment-combination of HDL_3 and $A\beta_{1-40}$ for 24 h as compared to control conditions. It remains to be investigated if ABCG1 aids in the proposed function of HDL to bind / scavenge Aβ peptides and/or in increased transport of Aβ across the BBB. In addition, increased ABCG1 expression may support anti-inflammatory functions of HDL at the BBB when challenged with Aβ.

Moreover, mRNA expression levels of lipoprotein related-receptor protein 1, LRP1, were determined via qRT-PCR. Recent *in vitro* studies showed that LRP1 promotes Aβ clearance across the BBB.[40] Storck *et al.* were able to confirm this theory in their *in vivo* studies using transgenic mouse strains (*Slco1c1-CreERT2 Lrp1fl/fl* mice) that allow tamoxifen-inducible deletion of *Lrp1* specifically within brain endothelial cells. A deletion of *Lrp1* resulted in strong reduction of Aβ efflux across the BBB.[41] HDL_3 treatment moderately (1.4-fold) and HDL_3 in combination with $A\beta_{1-40}$ substantially (2.1-fold) increased transcription of LRP1 in pBCEC. With this background information, increased levels of LRP1, ABCG1, and extracellular Aβ indicate that HDL_3 binds Aβ and promotes its transport across the BBB.

To substantiate this allegation, transport studies with our 3D BBB *in vitro* model were performed. Therefore, pBCEC were cultured on Transwell® filters in monolayers, where the basolateral side simulates brain parenchymal compartment while the apical side simulates the blood compartment. Contrary to expectations, these experiments did not reveal a significant difference in transport of $A\beta_{1-40}$ across pBCEC cultured on Transwells between vehicle control, HDL_3 and apoA-I, respectively, although these data must be interpreted with caution, because the transport experiments were performed only twice, using samples with relatively low TEER values, indicating that there was no proper formation of tight junctions.

To ensure that the results obtained so far were not misinterpreted and HDL_3 and apoA-I lead to uptake of Aβ by pBCEC, uptake studies were performed. Both, HDL_3 and apoA-I are accepted to bind Aβ and apoA-I coated particles were even shown to increase their uptake across the BBB.[96,105] Surprisingly, treatment with 2 µg/ml of apoA-I reduced the uptake of $Aβ_{1-40}$ by over 43%, treatment with 20 µg/ml by 19%. Studies of Forte *et al.* with apoA-I on Chinese hamster ovary (CHO) cell monolayers have shown that apoA-I has the ability to form extracellular assembly complexes with the sizes of the complex concentration-dependent. Thus, a higher concentration of apoA-I leads to bigger complexes.[106] One theory could be that small complexes of apoA-I and Aβ agglutinate and, thus, cannot enter the cells, while bigger complexes, containing more apoA-I stimulate the uptake of bound Aβ.

Increasing age leads to increased ROS levels, ROS have been linked to the pathogenesis of AD, and accumulation of Aβ peptides was consistently associated with increased ROS levels.[28–33] As previous *in vitro* studies have indicated, both HDL_3 and apoA-I contribute to inhibition of ROS formation,[107–109] with the data obtained in our studies we can infer that this theory also applies for pBCEC. ApoA-I and HDL may protect cerebrovascular cells from increased oxidative stress in the presence of Aβ.

Figure 12 summarizes the data obtained for HDL_3 treatment. In Figure 13 effects of apoA-I are illustrated.

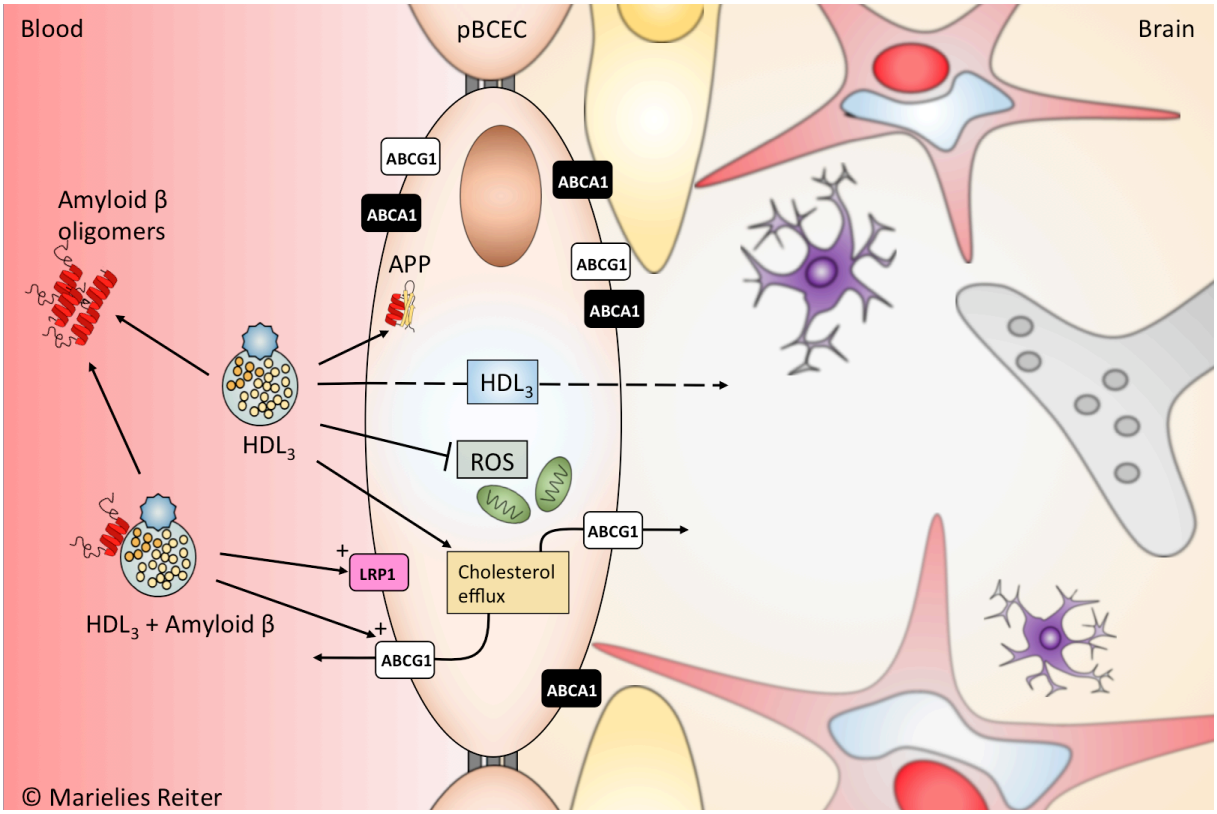

Figure 12: Effects of HDL_3 found in pBCEC. This schematic diagram illustrates a model of the BBB: pBCEC (brown) connected via tight junctions (dark grey), pericytes (yellow), astrocytes (red), microglia (purple) and neurons (grey) on the brain side. The scheme summarizes the effects of HDL_3 on pBCEC as revealed in our studies. We were able to prove that HDL_3 prevents ROS formation in pBCEC. Moreover, due to the results obtained we infer that HDL_3 leads not only to increased cholesterol efflux, preferably to the brain parenchymal side,[42] but also to upregulation of LRP1 mRNA levels, indicating that HDL_3 promotes Aβ transport out of the cells. In presence of Aβ, HDL_3 even leads to higher increased LRP1 mRNA levels and also increased ABCG1 mRNA levels. 24 h treatment with HDL_3 and HDL_3 in combination with Aβ, respectively, also revealed higher intracellular levels of APP protein, presently unclear whether these are further processed to sAPPα or Aβ. The finding of increased extracellular Aβ pre-fibrils in the environment could support the thesis that HDL_3 increases Aβ transport from the cells to the medium, possibly by binding it.

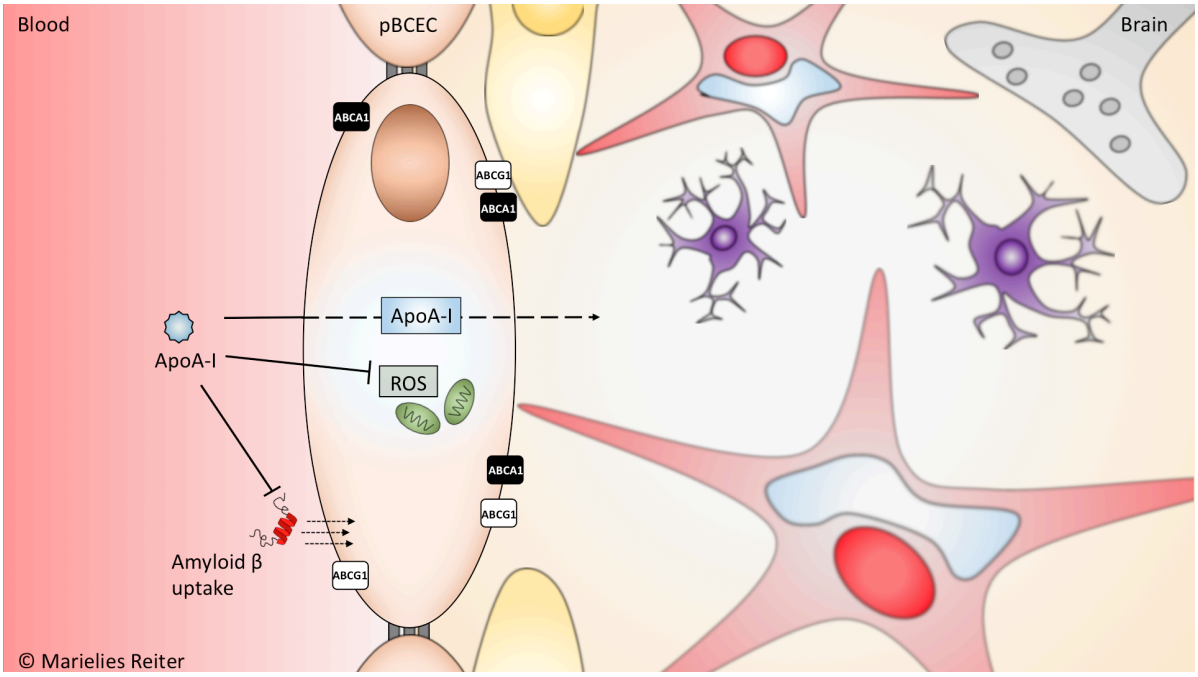

Figure 13: Effects found after 24h treatment with apoA-I. The scheme of the BBB shows pBCEC (brown) connected via tight junctions (dark grey), pericytes (yellow), astrocytes (red), microglia (purple) and neurons (grey) on the brain side. After treating pBCEC with apoA-I we found that apoA-I has the ability to inhibit ROS formation and, thus, prevents from oxidative stress. Also our results suggest that apoA-I counteracts Aβ uptake by BCEC.

In summary, the results of the present study indicate that HDL_3 in presence of Aβ upregulates LRP1 and ABCG1 transporter levels, suggesting a supporting function in the clearance and scavenging of Aβ peptides and oligomers. To date, it is unclear whether this effect is achieved by binding the peptides or by activating different clearance pathways. Moreover, further research is required to understand if the increase in APP protein levels leads to formation of beneficial sAPPα or crucial Aβ. Also, the ability of apoA-I to prevent Aβ uptake by pBCEC was proven, but it needs to be clarified if this process is concentration dependent. However, we found that both HDL_3 and apoA-I prevent ROS formation and maintain their potential as cholesterol acceptors in primary capillary endothelial cells when challenged with Aβ peptides.

6. Outlook

To gain further insights into APP processing at the BBB, the activity of BACE1 should be investigated with an activity assay. Also we would recommend redoing the transport study, using samples with TEER values of 300 and higher only. Protein levels of ABCG1 and LRP1 should be determined after treatment. The *in vitro* BBB model would also be suitable to determine in which direction cholesterol efflux in the presence of Aβ is promoted.

Concerning the uptake studies, apoA-I concentrations of 50 µg/ml and higher could be applied to see, if the Aβ uptake is in fact concentration-dependent.

We further aim to investigate if higher concentrations of HDL_3 as used here will lower Aβ oligomers in pBCEC and we would like to prove that HDL_3 binds Aβ oligomers and/or Aβ and determine the capacity of these bonds.

7. Indices

7.1. List of References

1. WHO. *Dementia*. (World Health Organization, 2015).

2. Alzheimer, A. Über eine eigenartige Erkrankung der Hirnrinde. *Allgemeine Zeitschrift fur Psychiatrie und Psychisch-gerichtliche Medizin* 146–8 (1907).

3. Ramirez-Bermudez, J. Alzheimer's disease: critical notes on the history of a medical concept. *Arch. Med. Res.* **43,** 595–599 (2012).

4. Huang, Y. & Mucke, L. Alzheimer mechanisms and therapeutic strategies. *Cell* **148,** 1204–1222 (2012).

5. Anand, R., Gill, K. D. & Mahdi, A. A. Therapeutics of Alzheimer's disease: Past, present and future. *Neuropharmacology* **76 Pt A,** 27–50 (2014).

6. Kivipelto, M. *et al.* Midlife vascular risk factors and Alzheimer's disease in later life: longitudinal, population based study. *BMJ* **322,** 1447–1451 (2001).

7. Buckner, R. L. Memory and executive function in aging and AD: multiple factors that cause decline and reserve factors that compensate. *Neuron* **44,** 195–208 (2004).

8. Talwar, P. *et al.* Dissecting Complex and Multifactorial Nature of Alzheimer's Disease Pathogenesis: a Clinical, Genomic, and Systems Biology Perspective. *Mol. Neurobiol.* (2015). doi:10.1007/s12035-015-9390-0

9. Di Paolo, G. & Kim, T.-W. Linking lipids to Alzheimer's disease: cholesterol and beyond. *Nat. Rev. Neurosci.* **12,** 284–296 (2011).

10. Francis, P. T., Palmer, A. M., Snape, M. & Wilcock, G. K. The cholinergic hypothesis of Alzheimer's disease: a review of progress. *J. Neurol. Neurosurg. Psychiatry* **66,** 137–147 (1999).

11. Murphy, M. P. & LeVine, H. Alzheimer's disease and the amyloid-beta peptide. *J. Alzheimers Dis. JAD* **19,** 311–323 (2010).

12. Kumar, A., Singh, A. & Ekavali, null. A review on Alzheimer's disease pathophysiology and its management: an update. *Pharmacol. Rep. PR* **67,** 195–203 (2015).

13. Christensen, M. A. *et al.* Transcriptional regulation of BACE1, the beta-amyloid precursor protein beta-secretase, by Sp1. *Mol. Cell. Biol.* **24,** 865–874 (2004).

14. Kojro, E. & Fahrenholz, F. The non-amyloidogenic pathway: structure and function of alpha-secretases. *Subcell. Biochem.* **38,** 105–127 (2005).

15. LaFerla, F. M., Green, K. N. & Oddo, S. Intracellular amyloid-beta in Alzheimer's disease. *Nat. Rev. Neurosci.* **8,** 499–509 (2007).

16. Hardy, J. A. & Higgins, G. A. Alzheimer's disease: the amyloid cascade hypothesis. *Science* **256,** 184–185 (1992).

17. Bush, A. I. The metallobiology of Alzheimer's disease. *Trends Neurosci.* **26,** 207–214 (2003).

18. Musiek, E. S. & Holtzman, D. M. Three dimensions of the amyloid hypothesis: time, space and 'wingmen'. *Nat. Neurosci.* **18,** 800–806 (2015).

19. Busciglio, J., Lorenzo, A., Yeh, J. & Yankner, B. A. beta-amyloid fibrils induce tau phosphorylation and loss of microtubule binding. *Neuron* **14,** 879–888 (1995).

20. Pérez, M., Cuadros, R., Benítez, M. J. & Jiménez, J. S. Interaction of Alzheimer's disease amyloid beta peptide fragment 25-35 with tau protein, and with a tau peptide containing the microtubule binding domain. *J. Alzheimers Dis. JAD* **6,** 461–467 (2004).

21. Hensley, K. *et al.* A model for beta-amyloid aggregation and neurotoxicity based on free radical generation by the peptide: relevance to Alzheimer disease. *Proc. Natl. Acad. Sci. U. S. A.* **91,** 3270–3274 (1994).

22. Reddy, P. H. & Beal, M. F. Amyloid beta, mitochondrial dysfunction and synaptic damage: implications for cognitive decline in aging and Alzheimer's disease. *Trends Mol. Med.* **14,** 45–53 (2008).

23. Mori, H., Takio, K., Ogawara, M. & Selkoe, D. J. Mass spectrometry of purified amyloid beta protein in Alzheimer's disease. *J. Biol. Chem.* **267,** 17082–17086 (1992).

24. Tarasoff-Conway, J. M. *et al.* Clearance systems in the brain-implications for Alzheimer disease. *Nat. Rev. Neurol.* **11,** 457–470 (2015).

25. Nathan, C. & Ding, A. SnapShot: Reactive Oxygen Intermediates (ROI). *Cell* **140,** 951–951.e2 (2010).

26. Nathan, C. & Cunningham-Bussel, A. Beyond oxidative stress: an immunologist's guide to reactive oxygen species. *Nat. Rev. Immunol.* **13,** 349–361 (2013).

27. Uttara, B., Singh, A. V., Zamboni, P. & Mahajan, R. T. Oxidative stress and neurodegenerative diseases: a review of upstream and downstream antioxidant therapeutic options. *Curr. Neuropharmacol.* **7,** 65–74 (2009).

28. Mattson, M. P. Cellular actions of beta-amyloid precursor protein and its soluble and fibrillogenic derivatives. *Physiol. Rev.* **77,** 1081–1132 (1997).

29. Matsuoka, Y., Picciano, M., La Francois, J. & Duff, K. Fibrillar beta-amyloid evokes oxidative damage in a transgenic mouse model of Alzheimer's disease. *Neuroscience* **104,** 609–613 (2001).

30. Smith, M. A. *et al.* Amyloid-beta deposition in Alzheimer transgenic mice is associated with oxidative stress. *J. Neurochem.* **70,** 2212–2215 (1998).

31. Mohmmad Abdul, H. *et al.* Mutations in amyloid precursor protein and presenilin-1 genes increase the basal oxidative stress in murine neuronal cells and lead to increased sensitivity to oxidative stress mediated by amyloid beta-peptide (1-42), HO and kainic acid: implications for Alzheimer's disease. *J. Neurochem.* **96,** 1322–1335 (2006).

32. Manczak, M. *et al.* Mitochondria are a direct site of A beta accumulation in Alzheimer's disease neurons: implications for free radical generation and oxidative damage in disease progression. *Hum. Mol. Genet.* **15,** 1437–1449 (2006).

33. De Felice, F. G. *et al.* Abeta oligomers induce neuronal oxidative stress through an N-methyl-D-aspartate receptor-dependent mechanism that is blocked by the Alzheimer drug memantine. *J. Biol. Chem.* **282,** 11590–11601 (2007).

34. Behl, C., Davis, J. B., Lesley, R. & Schubert, D. Hydrogen peroxide mediates amyloid beta protein toxicity. *Cell* **77,** 817–827 (1994).

35. Kaur, U. *et al.* Reactive oxygen species, redox signaling and neuroinflammation in Alzheimer's disease: the NF-κB connection. *Curr. Top. Med. Chem.* **15,** 446–457 (2015).

36. Shibata, M. *et al.* Clearance of Alzheimer's amyloid-ss(1-40) peptide from brain by LDL receptor-related protein-1 at the blood-brain barrier. *J. Clin. Invest.* **106,** 1489–1499 (2000).

37. Hermann, D. M. & ElAli, A. The abluminal endothelial membrane in neurovascular remodeling in health and disease. *Sci. Signal.* **5,** re4 (2012).

38. Wong, A. D. *et al.* The blood-brain barrier: an engineering perspective. *Front. Neuroengineering* **6,** 7 (2013).

39. Ujiie, M., Dickstein, D. L., Carlow, D. A. & Jefferies, W. A. Blood-brain barrier permeability precedes senile plaque formation in an Alzheimer disease model. *Microcirc. N. Y. N 1994* **10,** 463–470 (2003).

40. Kanekiyo, T. *et al.* Neuronal clearance of amyloid-β by endocytic receptor LRP1. *J. Neurosci. Off. J. Soc. Neurosci.* **33,** 19276–19283 (2013).

41. Storck, S. E. *et al.* Endothelial LRP1 transports amyloid-β1-42 across the blood-brain barrier. *J. Clin. Invest.* **126,** 123–136 (2016).

42. Panzenboeck, U. *et al.* ABCA1 and scavenger receptor class B, type I, are modulators of reverse sterol transport at an in vitro blood-brain barrier constituted of porcine brain capillary endothelial cells. *J. Biol. Chem.* **277,** 42781–42789 (2002).

43. Akanuma, S. *et al.* ATP-binding cassette transporter A1 (ABCA1) deficiency does not attenuate the brain-to-blood efflux transport of human amyloid-beta peptide (1-40) at the blood-brain barrier. *Neurochem. Int.* **52,** 956–961 (2008).

44. Elali, A. & Rivest, S. The role of ABCB1 and ABCA1 in beta-amyloid clearance at the neurovascular unit in Alzheimer's disease. *Front. Physiol.* **4,** 45 (2013).

45. Alzheimer, A. Über eigenartige Krankheitsfälle des späteren Alters. *Z. Für Gesamte Neurol. Psychiatr.* **4,** 356–385 (1911).

46. Corder, E. H. *et al.* Gene dose of apolipoprotein E type 4 allele and the risk of Alzheimer's disease in late onset families. *Science* **261,** 921–923 (1993).

47. Bertram, L. & Tanzi, R. E. Thirty years of Alzheimer's disease genetics: the implications

of systematic meta-analyses. *Nat. Rev. Neurosci.* **9,** 768–778 (2008).

48. Kim, J., Basak, J. M. & Holtzman, D. M. The role of apolipoprotein E in Alzheimer's disease. *Neuron* **63,** 287–303 (2009).

49. Bu, G. Apolipoprotein E and its receptors in Alzheimer's disease: pathways, pathogenesis and therapy. *Nat. Rev. Neurosci.* **10,** 333–344 (2009).

50. Pfrieger, F. W. Cholesterol homeostasis and function in neurons of the central nervous system. *Cell. Mol. Life Sci. CMLS* **60,** 1158–1171 (2003).

51. Ledesma, M. D. & Dotti, C. G. Amyloid excess in Alzheimer's disease: what is cholesterol to be blamed for? *FEBS Lett.* **580,** 5525–5532 (2006).

52. Dietschy, J. M. Central nervous system: cholesterol turnover, brain development and neurodegeneration. *Biol. Chem.* **390,** 287–293 (2009).

53. Shobab, L. A., Hsiung, G.-Y. R. & Feldman, H. H. Cholesterol in Alzheimer's disease. *Lancet Neurol.* **4,** 841–852 (2005).

54. Brown, M. S. & Goldstein, J. L. The SREBP pathway: regulation of cholesterol metabolism by proteolysis of a membrane-bound transcription factor. *Cell* **89,** 331–340 (1997).

55. Lund, E. G., Guileyardo, J. M. & Russell, D. W. cDNA cloning of cholesterol 24-hydroxylase, a mediator of cholesterol homeostasis in the brain. *Proc. Natl. Acad. Sci. U. S. A.* **96,** 7238–7243 (1999).

56. Björkhem, I., Lütjohann, D., Breuer, O., Sakinis, A. & Wennmalm, A. Importance of a novel oxidative mechanism for elimination of brain cholesterol. Turnover of cholesterol and 24(S)-hydroxycholesterol in rat brain as measured with 18O2 techniques in vivo and in vitro. *J. Biol. Chem.* **272,** 30178–30184 (1997).

57. Baranowski, M. Biological role of liver X receptors. *J. Physiol. Pharmacol. Off. J. Pol. Physiol. Soc.* **59 Suppl 7,** 31–55 (2008).

58. Panzenboeck, U. *et al.* Regulatory effects of synthetic liver X receptor- and peroxisome-proliferator activated receptor agonists on sterol transport pathways in polarized cerebrovascular endothelial cells. *Int. J. Biochem. Cell Biol.* **38,** 1314–1329 (2006).

59. Kim, W. S. *et al.* Role of ABCG1 and ABCA1 in regulation of neuronal cholesterol efflux to apolipoprotein E discs and suppression of amyloid-beta peptide generation. *J. Biol. Chem.* **282,** 2851–2861 (2007).

60. Cavelier, C., Lorenzi, I., Rohrer, L. & von Eckardstein, A. Lipid efflux by the ATP-binding cassette transporters ABCA1 and ABCG1. *Biochim. Biophys. Acta* **1761,** 655–666 (2006).

61. Duffy, D. & Rader, D. J. Update on strategies to increase HDL quantity and function. *Nat. Rev. Cardiol.* **6,** 455–463 (2009).

62. Chang, T.-Y., Chang, C. C. Y., Ohgami, N. & Yamauchi, Y. Cholesterol sensing, trafficking, and esterification. *Annu. Rev. Cell Dev. Biol.* **22,** 129–157 (2006).

63. Hutter-Paier, B. *et al.* The ACAT inhibitor CP-113,818 markedly reduces amyloid pathology in a mouse model of Alzheimer's disease. *Neuron* **44,** 227–238 (2004).

64. Puglielli, L. *et al.* Acyl-coenzyme A: cholesterol acyltransferase modulates the generation of the amyloid beta-peptide. *Nat. Cell Biol.* **3,** 905–912 (2001).

65. Shibuya, Y. *et al.* Acyl-coenzyme A:cholesterol acyltransferase 1 blockage enhances autophagy in the neurons of triple transgenic Alzheimer's disease mouse and reduces human P301L-tau content at the presymptomatic stage. *Neurobiol. Aging* **36,** 2248–2259 (2015).

66. Shibuya, Y., Chang, C. C. Y., Huang, L.-H., Bryleva, E. Y. & Chang, T.-Y. Inhibiting ACAT1/SOAT1 in microglia stimulates autophagy-mediated lysosomal proteolysis and increases Aβ1-42 clearance. *J. Neurosci. Off. J. Soc. Neurosci.* **34,** 14484–14501 (2014).

67. Murphy, S. R. *et al.* Acat1 knockdown gene therapy decreases amyloid-β in a mouse model of Alzheimer's disease. *Mol. Ther. J. Am. Soc. Gene Ther.* **21,** 1497–1506 (2013).

68. Kontush, A. *et al.* Structure of HDL: particle subclasses and molecular components. *Handb. Exp. Pharmacol.* **224,** 3–51 (2015).

69. McGrowder, D., Riley, C., Morrison, E. Y. S. A. & Gordon, L. The role of high-density lipoproteins in reducing the risk of vascular diseases, neurogenerative disorders, and cancer. *Cholesterol* **2011,** 496925 (2011).

70. Reitz, C. *et al.* Association of higher levels of high-density lipoprotein cholesterol in elderly individuals and lower risk of late-onset Alzheimer disease. *Arch. Neurol.* **67,** 1491–1497 (2010).

71. van Exel, E. *et al.* Association between high-density lipoprotein and cognitive impairment in the oldest old. *Ann. Neurol.* **51,** 716–721 (2002).

72. Muckle, T. J. & Roy, J. R. High-density lipoprotein cholesterol in differential diagnosis of senile dementia. *Lancet Lond. Engl.* **1,** 1191–1193 (1985).

73. Merched, A., Xia, Y., Visvikis, S., Serot, J. M. & Siest, G. Decreased high-density lipoprotein cholesterol and serum apolipoprotein AI concentrations are highly correlated with the severity of Alzheimer's disease. *Neurobiol. Aging* **21,** 27–30 (2000).

74. Gu, F. *et al.* Structures of discoidal high density lipoproteins: a combined computational-experimental approach. *J. Biol. Chem.* **285,** 4652–4665 (2010).

75. Vollbach, H. *et al.* APOA1 polymorphism influences risk for early-onset nonfamiliar AD. *Ann. Neurol.* **58,** 436–441 (2005).

76. Smach, M. A. *et al.* Polymorphism in apoA1 Influences High-Density Lipoprotein Cholesterol Levels but Is Not a Major Risk Factor of Alzheimer's Disease. *Dement. Geriatr. Cogn. Disord. Extra* **1,** 249–257 (2011).

77. Khalil, A., Berrougui, H., Pawelec, G. & Fulop, T. Impairment of the ABCA1 and SR-BI-mediated cholesterol efflux pathways and HDL anti-inflammatory activity in Alzheimer's disease. *Mech. Ageing Dev.* **133,** 20–29 (2012).

78. Ehrlich, P. *Das Sauerstoff-Bedürfnis des Organismus. Eine farbenanalytische Studie*. (August Hirschwald, 1885).

79. Rubin, L. L. & Staddon, J. M. The cell biology of the blood-brain barrier. *Annu. Rev. Neurosci.* **22,** 11–28 (1999).

80. Ueno, M. Molecular anatomy of the brain endothelial barrier: an overview of the distributional features. *Curr. Med. Chem.* **14,** 1199–1206 (2007).

81. Pardridge, W. M. Blood-brain barrier delivery. *Drug Discov. Today* **12,** 54–61 (2007).

82. Gerstner, E. R. *et al.* VEGF inhibitors in the treatment of cerebral edema in patients with brain cancer. *Nat. Rev. Clin. Oncol.* **6,** 229–236 (2009).

83. Stamatovic, S. M., Keep, R. F. & Andjelkovic, A. V. Brain endothelial cell-cell junctions: how to 'open' the blood brain barrier. *Curr. Neuropharmacol.* **6,** 179–192 (2008).

84. Schweinzer, C. K. Processing of APP in cerebrovascular endothelial cells - regulation by LXR agonists and altered cholesterol homeostasis. (Medical University of Graz, 2011).

85. Chirackal Manavalan, A. P. *et al.* Phospholipid transfer protein is expressed in cerebrovascular endothelial cells and involved in high density lipoprotein biogenesis and remodeling at the blood-brain barrier. *J. Biol. Chem.* **289,** 4683–4698 (2014).

86. Wahrle, S. E. *et al.* Overexpression of ABCA1 reduces amyloid deposition in the PDAPP mouse model of Alzheimer disease. *J. Clin. Invest.* **118,** 671–682 (2008).

87. Olesen, O. F. & Dagø, L. High density lipoprotein inhibits assembly of amyloid beta-peptides into fibrils. *Biochem. Biophys. Res. Commun.* **270,** 62–66 (2000).

88. Kontush, A. Apolipoprotein Abeta: black sheep in a good family. *Brain Pathol. Zurich Switz.* **14,** 433–447 (2004).

89. Hirsch-Reinshagen, V. *et al.* The absence of ABCA1 decreases soluble ApoE levels but does not diminish amyloid deposition in two murine models of Alzheimer disease. *J. Biol. Chem.* **280,** 43243–43256 (2005).

90. Koldamova, R., Staufenbiel, M. & Lefterov, I. Lack of ABCA1 considerably decreases brain ApoE level and increases amyloid deposition in APP23 mice. *J. Biol. Chem.* **280,** 43224–43235 (2005).

91. Koldamova, R., Fitz, N. F. & Lefterov, I. The role of ATP-binding cassette transporter A1 in Alzheimer's disease and neurodegeneration. *Biochim. Biophys. Acta* **1801,** 824–830 (2010).

92. Wahrle, S. E. *et al.* Deletion of Abca1 increases Abeta deposition in the PDAPP transgenic mouse model of Alzheimer disease. *J. Biol. Chem.* **280,** 43236–43242 (2005).

93. Litten-Brown, J. C., Corson, A. M. & Clarke, L. Porcine models for the metabolic syndrome, digestive and bone disorders: a general overview. *Anim. Int. J. Anim. Biosci.* **4,** 899–920 (2010).

94. Franke, H., Galla, H. & Beuckmann, C. T. Primary cultures of brain microvessel

endothelial cells: a valid and flexible model to study drug transport through the blood-brain barrier in vitro. *Brain Res. Brain Res. Protoc.* **5,** 248–256 (2000).

95. Sattler, W., Mohr, D. & Stocker, R. Rapid isolation of lipoproteins and assessment of their peroxidation by high-performance liquid chromatography postcolumn chemiluminescence. *Methods Enzymol.* **233,** 469–489 (1994).

96. Kratzer, I. *et al.* Apolipoprotein A-I coating of protamine-oligonucleotide nanoparticles increases particle uptake and transcytosis in an in vitro model of the blood-brain barrier. *J. Control. Release Off. J. Control. Release Soc.* **117,** 301–311 (2007).

97. Laemmli, U. K. Cleavage of structural proteins during the assembly of the head of bacteriophage T4. *Nature* **227,** 680–685 (1970).

98. Livak, K. J. & Schmittgen, T. D. Analysis of relative gene expression data using real-time quantitative PCR and the 2(-Delta Delta C(T)) Method. *Methods San Diego Calif* **25,** 402–408 (2001).

99. Glenner, G. G. & Wong, C. W. Alzheimer's disease: initial report of the purification and characterization of a novel cerebrovascular amyloid protein. *Biochem. Biophys. Res. Commun.* **120,** 885–890 (1984).

100. Rushworth, J. V. & Hooper, N. M. Lipid Rafts: Linking Alzheimer's Amyloid-β Production, Aggregation, and Toxicity at Neuronal Membranes. *Int. J. Alzheimers Dis.* **2011,** 603052 (2010).

101. Ferreira, S. T. & Klein, W. L. The Aβ oligomer hypothesis for synapse failure and memory loss in Alzheimer's disease. *Neurobiol. Learn. Mem.* **96,** 529–543 (2011).

102. Cerf, E. *et al.* Antiparallel beta-sheet: a signature structure of the oligomeric amyloid beta-peptide. *Biochem. J.* **421,** 415–423 (2009).

103. Kennedy, M. A. *et al.* ABCG1 has a critical role in mediating cholesterol efflux to HDL and preventing cellular lipid accumulation. *Cell Metab.* **1,** 121–131 (2005).

104. Umemoto, T. *et al.* Apolipoprotein AI and high-density lipoprotein have anti-inflammatory effects on adipocytes via cholesterol transporters: ATP-binding cassette A-1, ATP-binding cassette G-1, and scavenger receptor B-1. *Circ. Res.* **112,** 1345–1354 (2013).

105. Koudinov, A., Matsubara, E., Frangione, B. & Ghiso, J. The soluble form of Alzheimer's amyloid beta protein is complexed to high density lipoprotein 3 and very high density lipoprotein in normal human plasma. *Biochem. Biophys. Res. Commun.* **205,** 1164–1171 (1994).

106. Forte, T. M., Goth-Goldstein, R., Nordhausen, R. W. & McCall, M. R. Apolipoprotein A-I-cell membrane interaction: extracellular assembly of heterogeneous nascent HDL particles. *J. Lipid Res.* **34,** 317–324 (1993).

107. Mao, J., Liu, W. & Wang, Y. Apolipoprotein A-I expression suppresses COX-2 expression by reducing reactive oxygen species in hepatocytes. *Biochem. Biophys. Res. Commun.* **454,** 359–363 (2014).

108. Robbesyn, F. *et al.* HDL counterbalance the proinflammatory effect of oxidized LDL by inhibiting intracellular reactive oxygen species rise, proteasome activation, and subsequent NF-kappaB activation in smooth muscle cells. *FASEB J. Off. Publ. Fed. Am. Soc. Exp. Biol.* **17,** 743–745 (2003).

109. Terasaka, N. *et al.* ABCG1 and HDL protect against endothelial dysfunction in mice fed a high-cholesterol diet. *J. Clin. Invest.* **118,** 3701–3713 (2008).

7.2. List of Figures

7.3. List of Tables